PETROLOGICAL STUDIES OF THE YAMATO METEORITES
PART 1. MINERALOGY OF THE YAMATO METEORITES

Akihiko OKADA*

Abstract: In 1969, the 10th Japanese Antarctic Research Expedition Team collected nine stones lying on the glacier in the southeastern area of the Yamato Mountains, Antarctica (70°S, 37°E). By the mass-spectrometric study of rare gas and the chemical analysis of the stones, SHIMA, SHIMA and HINTENBERGER (1973) found four of them to be meteorites, and named them the Yamato (a), Yamato (b), Yamato (c) and Yamato (d). The other five stones were also determined to be meteorites because of their chondritic structures, and were named the Yamato (e), Yamato (f), Yamato (g), Yamato (h) and Yamato (i). According to the chemical composition, the Yamato (a), Yamato (b), Yamato (c) and Yamato (d) were assigned to an enstatite chondrite, a calcium-poor achondrite, a type III carbonaceous chondrite and a high-iron group chondrite, respectively. In this work, the mineralogical properties of the Yamato (a), Yamato (b), Yamato (c), Yamato (d) and Yamato (g) were studied in detail. The texture of meteorites and the occurrence, content and optical property of minerals were optically investigated with the polarizing microscopy in both the transmitted and the reflected light. Chemical compositions of main silicate minerals, olivine and pyroxene, and the silica minerals of the Yamato (a), Yamato (b) and Yamato (c) were analyzed with the electron probe microanalyzer.

1. Introduction

Antarctica has been considered a suitable place for the search of the extraterrestrial materials (SHIMA and YABUKI, 1968). Cosmic dust has already been found in the Antarctic ice, and its physical and chemical properties have been extensively studied (SHIMA, 1966, 1970; SHIMA and YABUKI, 1968; SHIMA *et al.*, 1969; YABUKI *et al.*, 1969; SHIMA *et al.*, 1972). On the other hand, four samples of meteorites have already been found in Antarctica, that is, two iron meteorites (Lazarev and Neptune Mountains), one pallasite (Thiel Mountains) and one olivine-hypersthene chondrite (Adelie Land) (HEY, 1966). In 1969, the 10th Japanese Antarctic Research Expedition Team found nine stone lying on the glacier near the Yamato Mountains (70°S, 37°E) of Antarctica (YOSHIDA *et al.*, 1971). SHIMA, SHIMA and HINTENBERGER (1973) investigated the isotopic abundance of rare gases and the chemical composition of the four samples of the stones, and confirmed them to be meteorites by detecting the presence of spallogenic ^{3}He, ^{22}Ne and ^{38}Ar. These four stones were named Yamato (a), Yamato (b), Yamato (c) and Yamato (d) after their locality. According to their chemical composition, they were assigned to an enstatite chon-

* The Institute of Physical and Chemical Research, Hirosawa, Wako-shi, Saitama-ken.

drite, a calcium-poor achondrite, a Type III carbonaceous chondrite and an olivine-bronzite chondrite, respectively. The classification was confirmed by further detailed chemical investigations by SHIMA (1974). The chondritic properties of the Yamato (a), Yamato (c) and Yamato (d) meteorites were also proved by the presence of chondrules (SHIMA, OKADA and SHIMA, 1973, 1974). The other five stones show a chondritic structure, too, and they were named Yamato (e), Yamato (f), Yamato (g), Yamato (h) and Yamato (i). However, detailed mineralogical investigations of these meteorites have not yet been reported. This paper presents the result of the systematic studies of the texture and mineral composition of the Yamato (a), Yamato (b), Yamato (c), Yamato (d) and Yamato (g) meteorites.

2. Samples

The meteorites were collected on the glacier in the southeastern area of the Yamato Mountains in Antarctica on December 21–26, 1969 (Fig. 1). Nine meteorites which belong to different meteoritic species were collectively found in the

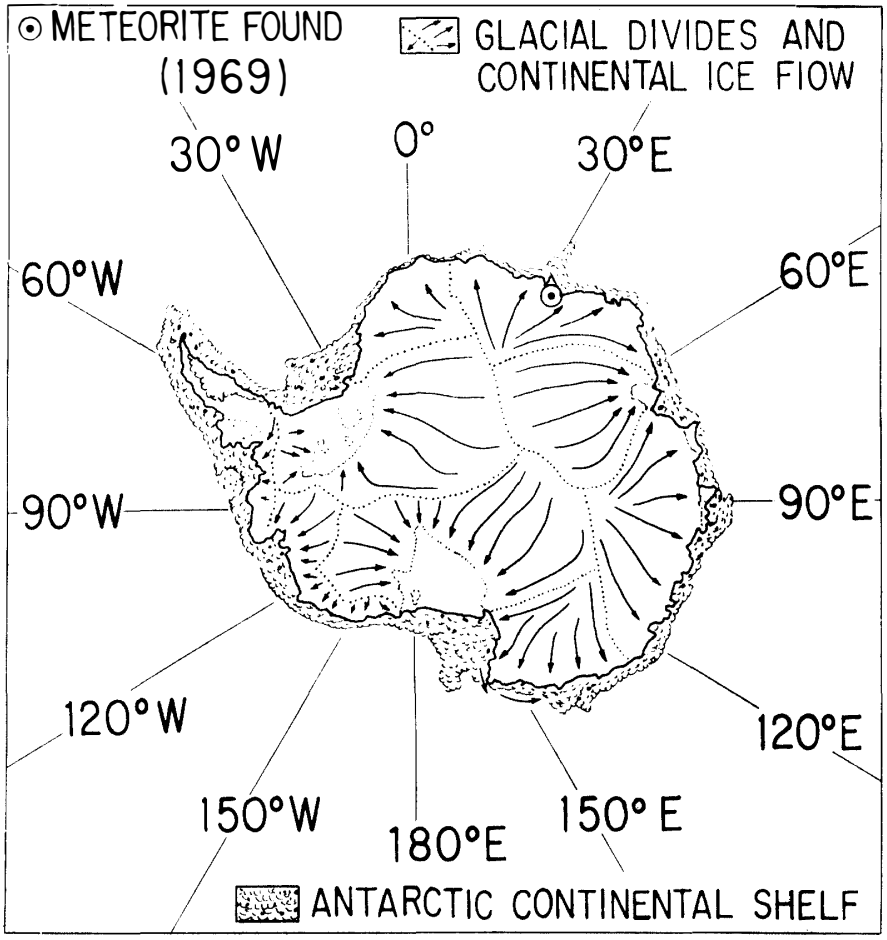

Fig. 1. Antarctica and the locality of the Yamato meteorites. The source of the figure is referred to SHIMA, SHIMA and HINTENBEGER (1973).

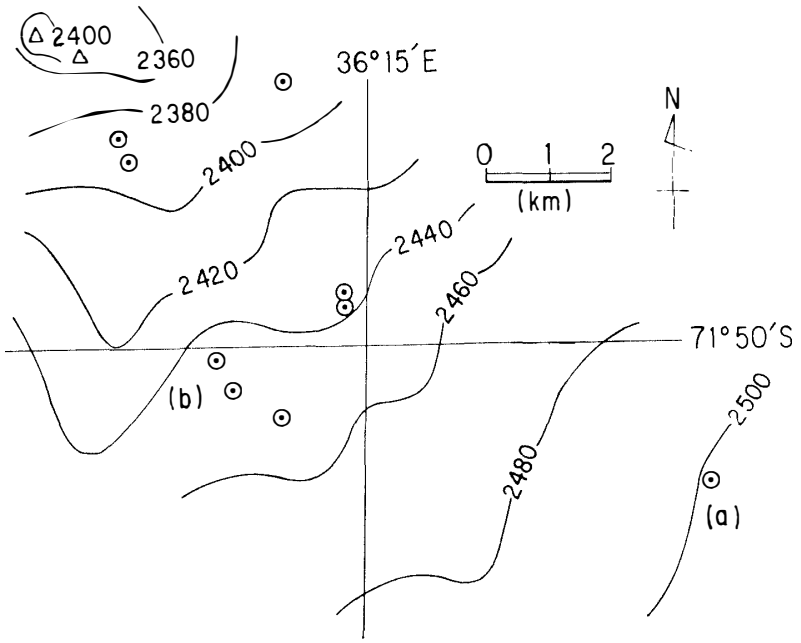

Fig. 2. The occurrence of the Yamato meteorites. They were found lying dispersedly on the glacier. The source of the figure is referred to YOSHIDA *et al. (1971).*

Table 1. Description of the samples.

Name	Classification*	Original weight (g)**	Original size** (in diameter, cm)	Description***	Date of find**
Yamato (a)	Enstatite chondrite	715	10	Thick black crust (1mm thick), dark-colored mass rich in metal phase, strong magnetic, chondritic.	Dec. 21, 1969
Yamato (b)	Ca-poor achondrite	138	7	Thin crust, non-chondritic	Dec. 21, 1969
Yamato (c)	Type III carbonaceous chondrite	150	5	Thick black crust (1mm thick), dark-colored mass, magnetic, chondritic.	Dec. 21–26, 1969
Yamato (d)	Olivine-bronzite chondrite	62	5	Thin crust, chondritic.	Dec. 21–26, 1969
Yamato (g)	Olivine-bronzite chondrite	25	5	Chondritic	Dec. 21–26, 1969

* SHIMA, SHIMA and HINTNBERGER (1973); SHIMA (1974).
** YOSHIDA *et al.* (1971).
*** SHIMA, OKADA and SHIMA (1973).

small area as shown in Fig. 2. In this work, the Yamato (a), Yamato (b), Yamato (c), Yamato (d) and Yamato (g) were investigated. Table 1 shows the brief description of the samples used in the present mineralogical studies. Thin sections

Table 2. Chemical composition[1] *and CIPW norm of the Yamato meteorites (wt. %).*

	Yamato			
	(a)	(b)	(c)	(d)
Silicate phase				
SiO_2	37.98	55.17	33.26	38.9
MgO	19.28	26.22	24.42	24.08
FeO	0.48	12.58	27.95[3]	12.32
Al_2O_3	1.55	0.70	2.44	1.93
CaO	0.45	1.21	2.37	1.68
Na_2O	0.864	0.0124	0.457	0.923
K_2O	0.0847	0.0059	0.0393	0.104
Cr_2O_3	0.418	1.375	0.564	0.498
MnO	0.247	0.515	0.173	0.302
TiO_2	0.075	0.072	0.133	0.082
P_2O_5	0.464	0.009	0.217	0.247
Metal phase				
Fe	22.18	0.66	0.06	12.45
Ni[2]	1.86	0.004	1.32	1.52
Co[3]	0.089	0.003	0.075	0.081
Sulfide phase				
Fe	7.20	0.85	2.30	3.38
Ca	0.72	—	—	—
S	4.71	0.489	1.32	1.94
Total Fe	29.75	11.29	24.09	25.41
Total	98.65	99.88	97.10	100.44

Norm

	(a)	(b)	(c)[5]	(d)
Q	3.48	4.03		
Or	0.56			0.56
Ab	7.34		3.67	7.86
An		1.95	4.73	0.83
Di Wo		1.74	2.21	2.44
Di En		1.21	1.31	1.61
Di Fs		0.40	0.79	0.66
Hy En	47.89	64.05	2.21	20.78
Hy Fs	0.92	22.30	1.19	7.52
Ol Fo			40.17	26.31
Ol Fa			24.96	10.60
Ap	0.91		0.62	0.62
Mt			9.49	
Cm	0.67	2.01	0.90	0.90
Il	0.15	0.15	0.30	0.15
Metal[4]	24.13	0.66	1.55	14.29
Troilite	11.34	1.34	3.62	5.32
Oldhamite	1.30			
Total	98.69	99.84	97.72	100.45

(1) SHIMA (1974).
(2) Total nickel and cobalt are listed as metal for convenience (SHIMA, 1974).
(3) More than half of oxide iron is present in the form of Fe_3O_4 (SHIMA, 1974).
(4) Normative metal.
(5) In the calculation of normative magnetite, Fe_2O_3 content of the Yamato (c) meteorite was estimated from the EPMA data of olivine.

for optical studies of transparent minerals were made for all meteorite samples. Polished thin sections for electron probe microanalysis and opaque mineral studies were also prepared for all samples but the Yamato (g) meteorite. A small part of each sample was pulverized for the X-ray studies and refractive index measurement. Table 2 shows the chemical compositions of the meteorites presented by SHIMA (1974) and the CIPW norms calculated from the data.

3. Experimental Method

3.1. Microscopic investigation

Microscopic examination of minerals was carried out on the thin sections and polished ones of the Yamato (a), Yamato (b), Yamato (c) and Yamato (d) meteorites under the transmitted and reflected light. The Yamato (g) meteorite was investigated only under the transmitted light. The physical properties of minerals were observed under the microscope. For the opaque minerals, the internal reflection and polishing hardness were also observed. For the main silicate minerals, the optical constants, refractive index, extinction angle, optic orientation, optic axial angle and optic sign, were investigated in detail. Refractive indices of olivine, pyroxene, plagioclase and silica minerals in the meteorite specimens were measured under the monochromatic light (589.3 mμ) by the oil immersion method at room temperature. The refractive index of the immersion liquid was always checked with the Abbe-type refractometer and Jelley-type one before and after the measurement of minerals. The expected error of the refractive index is ± 0.003.

Extinction angle, optic orientation, optic axial angle and optic sign of olivine, pyroxene, plagioclase and silica minerals of the Yamato (a), Yamato (b), Yamato (c), Yamato (d) and Yamato (g) meteorites were measured using a universal stage. The refraction correction was carried out using a diagram by SUWA and NAGASAWA (1961).

Modal compositions of minerals were measured with a point counter.

3.2. Electron probe microanalysis

The chemical compositions of olivine, pyroxene, plagioclase, silica minerals and glass of the Yamato (a), Yamato (b) and Yamato (c) were determined by the quantitative electron probe microanalyses. Polished thin sections of the meteorite samples were coated with carbon layer, a few hundred angstroms in thickness. The measurements were performed with the Japan Electron Optics Laboratory electron probe microanalyzer (JXA-5A) located at the Geological Survey of Japan. The sample was bombarded with a finely focused electron beam, about 2 micrometers in diameter, accelerated by high voltage, 15 kilovolts.

The wavelength and intensity of the resultant X-ray emission spectrum were analyzed with the dispersive X-ray detection systems. The chemical analyses of minerals were carried out by the following procedure. The grains were optically selected under the transmitted and reflected light with a microscope, and bombarded by the electron beam. The quantitative analyses of elements,

Na, K, Ti, Mn, Si, Mg, Fe, Ca and Al, were carried out on every grain. Chemically analyzed oxide and silicate minerals were used as standards. They are jadeite for Na, adularia for K, rutile for Ti, rhodonite for Mn, quartz for Si, periclase for Mg, hematite for Fe, wollastonite for Ca and corundum for Al. The quantitative data were corrected for wavelength shift, deadtime, background, mass absorption, secondary fluorescence and atomic number according to the procedure by SWEATMAN and LONG (1970). Calculations were carried out using computer programs developed by OKUMURA and KAWACHI (1971), KAWACHI (1971) and NAKATSUKA (1974). The qualitative X-ray microanalyses were carried out for the identification of opaque minerals. The scanning images of the mineral grains were observed on a oscilloscope screen sweeping the electron beam over a selected area in the sample and recording the resultant characteristic X-ray intensities.

3.3. X-ray measurement

The measurements of cell dimensions of olivine and pyroxene of the Yamato (a), Yamato (b), Yamato (c) and Yamato (d) meteorites were made on the powdered samples with a D-9C X-ray Diffractometer (Rigaku Electric Co. Ltd.). The finely pulverized samples were diluted with ethylalcohol directly on the glass slide. After the evaporation of ethylalcohol, a smooth layer of sample was spread on the glass slide, Cu Kα line monochromatized by a LiF crystal was irradiated on the sample. The X-ray powder pattern was recorded from $2\theta=80°$ to $2\theta=10°$. The diffraction peaks of olivine and pyroxene were indexed with reference to the X-ray data of forsterite, enstatite, bronzite and clinoenstatite by HOWIE (1963), STEPHENSON *et al.* (1966) and JAHANBAGLOO (1969). The traverses were run at 4 minutes per degree (2θ) and a chart paper speed equivalent to 8 cm per degree. Pure quartz was used as the external standard. X-ray powder patterns of each sample and quartz were alternately measured five times, and the 2θ values of diffraction lines of the sample were corrected by those of quartz. The cell dimensions of olivine and pyroxene were calculated by the least square method.

The Debye-Scherrer photographs were also taken to ascertain the identification of opaque minerals. The mineral grains picked up from the pulverized samples of the Yamato (a), Yamato (b), Yamato (c) and Yamato (d) meteorites under the microscope were finely crushed and mounted on the thin glass rod, about 0.1 mm in diameter. The Debye-Scherrer patterns were taken by the filtered Fe Kα radiation under the condition of 30 kV and 10 mA, using a camera, 114.6 mm in diameter. The mineral species were identified with reference to the ASTM X-ray powder data.

4. Structure and Mineralogy

4.1. Yamato (a) meteorite

The Yamato (a) meteorite is black, hard and dense in appearance, and shows

Table 3. Modal composition of the Yamato (a) meteorite (vol. %).

Matrix	Orthopyroxene	38.5
	Clinopyroxene	21.3
	Olivine	3.7
	Cristobalite	0.4
	Glass	0.5
	Opaque minerals	35.6
Total		100.0
Chondrule	Orthopyroxene	52.0
	Clinopyroxene	32.4
	Olivine	4.2
	Plagioclase	1.1
	Cristobalite	0.1
	Spinel-like mineral	trace
	Glass	2.6
	Opaque minerals	6.9
	Others*	0.7
Total		100.0
Matrix		83.9
Chondrule		16.1
Total		100.0

* Cryptocrystalline materials.

a well-developed chondritic structure (Fig. 3). It is composed mainly of clinopyroxene (clinoenstatite), orthopyroxene (enstatite) and opaque minerals, with small amounts of olivine, plagioclase, cristobalite and glass. The modal composition of the Yamato (a) meteorite is shown in Table 3. In this meteorite, clinopyroxene is distinguished by the polysynthetic twinning, and orthopyroxene shows very strong undulatory extinction. The presence of glass and the coexistence of free silica (cristobalite) and orthopyroxene-rimmed olivine grains show that this meteorite was not in the equilibrium state. The opaque phase predominated by metallic nickel-iron and troilite occupies a large part of the meteorite, about 30 vol. %, and it contains several kinds of opaque minerals, graphite, daubreelite, schreibersite, perryite, Ca- and Cr-bearing (Mg, Fe, Mn)S and so on, which occur in intimate intergrowth with each other.

Chondrules, 0.03 to 3 mm in diameter, are dispersedly embedded in the dark-colored matrix, and occupy about 16 vol. % of the main mass. They are spheroidal, ovoid, ellipsoidal, pear-like and irregular in shape, and have distinct boundaries in the matrix. Granular-type chondrules which are polysomatically com-

posed of euhedral to subhedral pyroxene and olivine phenocrysts with small amounts of glass and opaque minerals are most common in this meteorite (Fig. 4). Colorless to pale brown glass is frequently found in the interstices among the silicate phenocrysts in these chondrules. In some chondrules, the interstitial glass is partially or wholly devitrified, changing to the dark brown fibrous material, probably pyroxene. The barred-type chondrules which consist of eccentrically radiated or parallel pyroxene layers are also abundant next to the granular chondrules (Fig. 5). Though small in amount and in size, the cryptocrystalline chondrules and cristobalite spherules are also noticeable. The cryptocrystalline chondrules, 0.05 to 0.2 mm in diameter, are pale brown or brownish yellow to dark brown in color, and show quite irregular wavy extinction (Fig. 6). Some of them show very finely fibrous crystallization with a radiated structure partially or wholly in their bodies. Cristobalite spherules, 0.03 to 0.1 mm in diameter, are colorless and look like glassy material (Fig. 7), but the spherules have very low birefringence in the polarized light under the higher magnification. Some spherules include a cryptocrystalline material in their bodies. In some chondrules with irregular shapes, the presence of broken and fragmentary chondrules is notable. Some of them are partly broken off in their margin (Fig. 8), and some assume the crescent to hemispheric forms (Fig. 9). Chondrule fragments which were more extensively collapsed are commonly found in the matrix of the Yamato (a) meteorite. This fact suggests that this meteorite is an unequilibrated one (REID and FREDRIKSSON, 1967). In addition to the above-described chondrules, a chondrule which is composed of eutectic-like aggregate of metallic nickel-iron layers interstitially filled with clinopyroxene and plagioclase is present in this meteorite (Fig. 10). Figure 11 shows a sheared chondrule fragment. Clinopyroxene and orthopyroxene are extremely sheared and folded by a strong stress. It is observed that pyroxene locally alters to minute droplet-like aggregates which are assumed to have been formed by the partial melting (Fig. 12). Another conspicuous feature of pyroxene chondrules is the presence of conglutinated individuals (Fig. 13). It is suggested that the original molten droplets joined in the stage of chondrule formation. Chondrule-like aggregates of opaque minerals are also found in the section of the meteorite. They are a complex aggregate of troilite, schreibersite, kamacite and (Mg, Fe, Mn, Ca, Cr)S with interstitial silicate grains, and a spheroidal form of a single troilite grain (Fig. 14).

The matrix, about 84 vol. % of the main mass, is dominated by clinopyroxene, orthopyroxene and opaque minerals which are mainly kamacite and troilite. Silicate grains are present in the forms of isolated single grains and aggregates which consist of pyroxene, olivine, cristobalite and glass. Opaque minerals are intimately intergrown with each other, filling the interstices among the silicate phase. Fine myrmekitic intergrowth of kamacite and troilite is one of the conspicuous textural features of opaque phase (Fig. 15). Such myrmekitic intergrowths are present in the forms of grains and veins in the limited part of the meteorite. They are often accompanied by the clusters of minute droplets of unmixed kamacite and troilite in the partially vitrified silicate phase (Fig. 16).

Another characteristic feature is the exsolution phenomenon in troilite (Fig. 17). In the reflected light, the exsolved mineral is slightly greenish in color, and completely isotropic, and is determined as daubreelite.

4.1.1. Pyroxene

Pyroxene is a dominant constituent of the silicate phase of the Yamato (a) meteorite. Orthopyroxene exhibits euhedral to subhedral crystal forms. The grains are colorless and range up to 0.3 mm in size. (110) cleavage and (100) parting are prominent in most grains, which are commonly traversed by irregular fractures. The optical properties of orthopyroxene are as follows:

Optic axial angle: $2V$ (aver.)$=+56°$ for the matrix orthopyroxene.
$=+57°$ for the orthopyroxene in chondrules.
Refractive index: $\alpha_D=1.654$, $\gamma_D=1.663$
Pleochroism: None

According to the determinative curve by KUNO (1954), the orthopyroxene is enstatite, and its molar composition is $En_{98}Fs_2$ for the matrix orthopyroxene and $En_{97}Fs_3$ for chondrule orthopyroxene. There is no remarkable difference in the composition of orthopyroxene between matrix and chondrules. In chondrules, orthopyroxene is always associated with clinopyroxene (clinoenstatite). In some cases, narrow bands of orthopyroxene are present in lamellar twinnings of clinopyroxene. This is recognized by the straight extinction in the lamellae in the polarized light. In this case, (100) plane and b-axis of orthopyroxene are parallel to those of clinopyroxene (Fig. 18). Remarkable characteristic of orthopyroxene in this meteorite is very strong undulatory extinction. The extinction sweeps irregularly across the crystal with the rotation of microscope stage. This may be ascribed to the slight movement which takes place along the cleavage or fracture, turning a single crystal into mosaic structure with slightly different orientations by stress or deformation (REID and COHEN, 1967).

In the polarized light, clinopyroxene is distinguishable by its polysynthetic twinning, in which each set of lamella shares (100) plane and b-axis with one another (Fig. 19). The euhedral to subhedral grains are colorless and 0.3 mm in maximum size. The optical properties and cell dimensions show that the clinopyroxene is clinoenstatite.

Optic axial angle: $2V$ (aver.)$=+52°$
Extinction angle: $c \wedge Z=23°$
Refractive index: $\alpha_D=1.653$, $\gamma_D=1.663$
Pleochroism: None
Unit cell parameters: $a=9.621\pm0.009$Å
$b=8.829\pm0.008$Å
$c=5.184\pm0.006$Å
$\beta=108.3°\pm0.1°$

Clinoenstatite is present in the enstatite chondrites which are the least recrystallized (MASON, 1966). Two kinds of pyroxene, enstatite and clinoenstatite, coexist in this meteorite. This association may be due to partial conversion of clinoenstatite

Table 4. Chemical composition of pyroxene in the Yamato (a) meteorite (wt. %).

Sample No.	SiO_2	TiO_2	Al_2O_3	FeO	MnO	MgO	CaO	Na_2O	K_2O	Total	Note
Orthopyroxene											
YA 18	60.01	0.01	0.18	1.07	0.08	38.41	0.18	0.02	0.01	99.97	Matrix
YA 20	60.53	0.08	0.37	0.42	0.22	38.65	0.30	0.02	0.00	100.58	Chondrule
YA 23	60.05	0.04	0.40	0.46	0.22	38.18	0.23	0.06	0.01	99.67	Chondrule
YA 27	60.44	0.11	0.41	0.63	0.07	39.18	0.32	0.03	0.01	101.20	Chondrule
YA 32	60.37	0.06	0.33	0.54	0.13	38.80	0.24	0.00	0.00	100.46	Chondrule
YA 36	60.24	0.08	0.46	0.61	0.09	38.27	0.36	0.00	0.00	100.12	Chondrule
Average	60.27	0.06	0.36	0.62	0.14	38.58	0.27	0.02	0.01	100.33	
Clinopyroxene											
YA 7	59.90	0.03	0.51	0.51	0.17	38.15	0.47	0.03	0.00	99.78	Chondrule
YA 16	59.20	0.00	0.56	0.88	0.06	37.98	0.44	0.08	0.00	99.21	Chondrule
YA 22	60.93	0.02	0.39	0.46	0.19	38.51	0.30	0.04	0.00	100.85	Chondrule
YA 26	60.53	0.10	0.65	0.42	0.20	38.23	0.40	0.02	0.00	100.56	Chondrule
YA 28	59.60	0.15	1.06	0.40	0.19	37.84	0.46	0.09	0.01	99.80	Chondrule
YA 37	60.70	0.05	0.26	1.05	0.10	38.65	0.20	0.02	0.00	100.98	Chondrule
Average	60.14	0.05	0.57	0.62	0.15	38.22	0.38	0.04	0.00	100.19	
Total Average	60.21	0.06	0.47	0.62	0.15	38.40	0.33	0.03	0.00	100.27	

Average structural formula

Orthopyroxene : $(Ca_{0.010}\ Na_{0.001})\ (Mg_{1.918}\ Fe_{0.002}\ Ti_{0.002}\ Mn_{0.004}\ Al_{0.016})\ Si_{2.011}O_6$

Clinopyroxene : $(Ca_{0.012}\ Na_{0.002})\ (Mg_{1.912}\ Fe_{0.018}\ Ti_{0.002}\ Mn_{0.004}\ Al_{0.020})\ Si_{2.010}O_6$

to more stable enstatite on cooling.

Another clinopyroxene found in the extremely sheared pyroxene chondrule is shown in Fig. 11. It is nonpleochroic and has extinction angle ($c \wedge Z$) of about 38°. However, its mineral species could not be identified because of the extremely sheared and folded structure, giving very strong wavy extinction.

Chemical compositions of pyroxenes are determined by electron probe micro-analyses (Table 4). The result shows that orthopyroxene and clinopyroxene are very low in FeO content, indicating nearly pure enstatite and clinoenstatite, respectively. The average contents of other minor constituents, TiO_2, Al_2O_3, MnO and CaO, also show lower values than those of terrestrial enstatite. In the enstatite chondrite, normally lithophile elements, Ca, Ti, V, Cr and Mn, have a tendency to become chalcophile, and occur in troilite or in other sulfides (ALLEN and MASON, 1973). Therefore, these elements are found in a fairly low content in the ferromagnesian silicates of the enstatite chondrite. MASON (1966) presented the wet chemical analysis of carefully separated enstatite of the Khairpur enstatite chondrite. The result shows higher contents of Al_2O_3 (1.18 wt. %) and Na_2O (0.174 wt. %). KEIL (1968) suggested that the result is probably due to the presence of minute plagioclase inclusions.

Though pyroxenes of the enstatite chondrite is Fe-poor enstatite and clinoenstatite, notable differences of the chemical composition were found within the enstatite chondrite group (KEIL, 1968). The chemical differences correspond to the subgroups of the enstatite chondrite, which were first proposed by ANDERS

Table 5. Average chemical compositions of pyroxenes (enstatite and clinoenstatite) of the Yamato (a) meteorite and type I, intermediate type and type II enstatite chondrites (wt. %).

	SiO_2	TiO_2	Al_2O_3	FeO	MnO	MgO	CaO	Na_2O	K_2O	Note
Yamato (a)	60.2	0.06	0.47	0.62	0.15	38.4	0.33	0.03	0.00	This work
Type I*	59.5	—	0.28	0.69	0.14	39.3	0.20	0.10	n.d.	KEIL (1968)
Intermediate type*	59.2	—	0.04	0.38	0.09	39.4	0.07	0.05	n.d.	Do.
Type II*	59.4	—	0.29	0.18	0.01	39.2	0.74	0.05	n.d.	Do.

* Type I Abee, Adhi Kot, Indarch and Kota Kota meteorites.
Intermediate type St. Marks and Saint Sauveur meteorites.
Type II Atlanta, Blithfield, Daniel's Kuil, Hvittis, Jajh deh Kot Lalu, Khairpur, Pillistfer and Ufana meteorites.

(1964) and MASON (1966) and established by KEIL (1968). They include a comparatively unrecrystallized enstatite chondrite (type I), a highly recrystallized one (type II) and an intermediate one between type I and type II. Table 5 shows the average chemical compositions of enstatite and clinoenstatite of each subgroup and the Yamato (a) meteorite. Generally, pyroxene of type I enstatite chondrite is higher in MnO, FeO and Na_2O contents and lower in CaO content than that of type II. Pyroxene of intermediate type enstatite is lower in Al_2O_3 and CaO contents than that of either type I or type II. As the result, pyroxene of the Yamato (a) seems to bear a resembrance to that of type I unrecrystallized enstatite chondrite.

4.1.2. Olivine

Olivine, a dominant constituent of the ordinary chondrites, is absent or present only in traces in the enstatite chondrite (MASON, 1966; BINNS, 1967; ALLEN and MASON, 1973). In the Yamato (a) meteorite, euhedral to subhedral grains of olivine are present in both the matrix and chondrules. The grains, 0.3 mm in maximum size, show undulatory extinction. The prismatic olivine grains are present surrounded by enstatite and clinoenstatite in the microporphyritic

Table 6. Chemical composition of olivine in the Yamato (a) meteorite and other enstatite chondrites** (wt. %)*

Sample No.	SiO_2	TiO_2	Al_2O_3	FeO	MnO	MgO	CaO	Na_2O	K_2O	Total
YA 3	43.48	0.02	0.06	0.83	0.12	56.33	0.15	0.00	0.00	100.99
YA 14	43.41	0.02	0.02	1.47	0.15	55.04	0.07	0.01	0.00	100.19
Indarch	43.5			0.4		58.4				102.3
Kota Kota	43.3			0.8		56.2				100.3

* Both grains, YA 3 and YA 14, are present in chondrules.
** BINNS (1967).
Structural formula: YA 3: $Ca_{0.004}(Mg_{1.952}Fe_{0.016}Mn_{0.002}Al_{0.002})Si_{1.011}O_4$
YA 14: $Ca_{0.002}(Mg_{1.928}Fe_{1.029}Mn_{0.003}Al_{0.001})Si_{1.018}O_4$

chondrules, and olivines are frequently in intimate contact with pale brown glass, partially devitrified. Subhedral olivines are also found in the chondrules composed mostly of radiatingly elongated rods of pyroxene (Fig. 20). In the matrix, olivine, exhibiting subhedral crystal forms, is frequently mantled by the reaction rim of enstatite (Fig. 21). The optical properties of olivine are as follows:

Optic axial angle: 2V (aver.)= +87° for the matrix olivine.
+84° for the olivine in chondrules.

Refractive index: $\alpha_D = 1.638$, $\gamma_D = 1.674$

The chemical composition of olivine determined by electron microprobe analysis is shown in Table 6. The average compositions of olivines in other enstatite chondrites are also given in the table (BINNS, 1967). The olivine in the enstatite chondrite is extremely low in iron content, and belongs to nearly pure forsterite. The average molar composition of forsterite component of olivines based on the microprobe data is $Fo_{98.9}$ in the Yamato (a) meteorite. On the other hand, BINNS (1967) reported $Fo_{99.2}$ in Kota Kota and $Fo_{99.6}$ in Indach. The enstatite-rimmed olivine is suggested to have been formed by the reaction between olivine and oversaturated liquid. On the other hand, in the CIPW norm in Table 2, olivine is not present, although silica is present. Therefore, olivine in the Yamato (a) meteorite would have disappeared, if the reaction between olivine and the liquid had proceeded further. The olivine-bearing enstatite chondrite, Kota Kota, Indarch and South Oman, have unrecrystallized textures (BINNS, 1967). The similar feature is noticed in the Yamato (a) meteorite.

4.1.3. Plagioclase

Plagioclase is rarely seen in the Yamato (a) meteorite, and it is nearly absent in the matrix. Minute grains of plagioclase twinned after albite law are present in the metallic chondrule as shown in Fig. 10, associated with clinopyroxene in the interstices among the alternate layers of metallic nickel-iron.

4.1.4. Cristobalite

In the Yamato (a) meteorite, free silica is present in the form of cristobalite. Colorless spherules, 0.03 to 0.1 mm in diameter, are unique in this meteorite (Fig. 7). They often have irregular or conchoidal fractures. In the polarized light, they are nearly isotropic, but show a very low birefringence under the higher magnification. Platy or needle-like crystals, less than 0.1 mm in size, are also found in the fibrous orthopyroxene aggregates, pale brown in color (Fig. 22). The average refractive index is $n_D = 1.485$. Electron probe data are shown

Table 7. Chemical composition of cristobalite in the Yamato (a) meteorite (wt. %).*

Sample No.	SiO_2	TiO_2	Al_2O_3	FeO	MnO	MgO	CaO	Na_2O	K_2O	Total
YA 12	99.27	0.00	0.17	0.31	0.03	0.01	0.03	0.02	0.00	99.85
YA 35	98.07	0.00	0.20	0.30	0.04	0.22	0.18	0.07	0.01	99.10

* YA 12 is a cristobalite spherule.
YA 35 is present in the fibrous pyroxene aggregate in the matrix.

in Table 7. Free silica comprising quartz, tridymite and cristobalite is commonly present in the enstatite chondrite (MASON, 1962a, 1966). Correlations between silica polymorphism and the texture of the enstatite chondrite were described by MASON (1966), BINNS (1967) and KEIL (1968). Quartz is present in the recrystallized and intermediate-type enstatite chondrites. Tridymite occurs in both unrecrystallized and recrystallized enstatite chondrites. Cristobalite exists in the unrecrystallized and intermediate-type enstatite chondrites. In the Yamato (a) meteorite, cristobalite spherules have micron-sized silicate inclusions, and sometimes much larger ones. KEIL (1968) showed that free silica includes minute grains of troilite, niningerite and daubreelite in several enstatite chondrites.

4.1.5. Glass and devitrified glass

Glass is present in various forms and sizes, interstitially filling the space of silicate aggregates in the matrix and chondrules. The degree of devitrification

Table 8. Chemical composition and CIPW norm of glass and devitrified glass in the Yamato (a) meteorite (wt. %).

Sample No.	Glass*	Devitrified glass*		
	YA 2	YA 17	YA 5	YA 21
SiO_2	69.21	66.03	60.54	61.86
TiO_2	0.69	0.47	0.61	0.57
Al_2O_3	15.43	17.85	17.71	16.78
FeO	0.35	0.20	0.33	0.41
MnO	0.00	0.00	0.50	0.24
MgO	10.07	10.02	6.08	7.31
CaO	0.31	0.49	11.77	8.48
Na_2O	3.57	4.07	3.05	3.09
K_2O	1.49	0.70	0.28	0.35
Total	101.12	99.83	100.85	99.09
Norm				
Q	26.79	23.73	12.49	15.62
C	7.23	9.48	—	—
Or	8.90	3.89	1.67	2.22
Ab	30.41	34.61	25.69	26.22
An	1.66	2.50	33.94	30.88
Di Wo	—	—	10.22	4.64
Di En	—	—	8.63	4.01
Di Fs	—	—	0.26	—
Hy En	25.09	24.99	6.52	14.15
Hy Fs	—	—	0.26	0.26
Il	0.75	0.45	1.21	1.06
Ru	0.31	0.23	—	—
Total	101.14	99.88	100.89	99.06

* YA 2 is pale brown, isotropic glass, surrounded by olivine grains. YA 17 is slightly devitrified glass, violet brown in color, surrounded by pyroxene. YA 5 is brown-colored devitrified glass, surrounded by pyroxene. YA 21 is finely devitrified glass, changing to a dark brown, fibrous material.

of glassy material is various, from the isotropic, pale brown glass to the finely devitrified ones, changing into brownish to dark brown fibrous materials, probably pyroxene (Fig. 23). In some glasses, the crystallization of euhedral, needle-like pyroxene is observed as shown in Fig. 24. Minute grains of spinel-like minerals, 0.001 to 0.004 mm in size, are found in the pale brown, partially devitrified glass in some chondrules (Fig. 25). The grains are isotropic and greenish under the microscope. Skeletal crystallites of dendritic growth, 0.004 to 0.01 mm in size and green in color, are present associated with spinel-like crystals (Fig. 26). The interstitial glass, including devitrified one, was analyzed with electron probe microanalyzer (Table 8). The samples are all interstitial glass and devitrified glass surrounded by olivine and pyroxene in the microporphyritic chondrules. Two types of glasses are present. YA2 and YA17 glasses are higher in SiO_2, MgO, Na_2O and K_2O contents and distinctly lower in CaO content than others, YA5 and YA21. In CIPW norms, the former type is higher in normative quartz, corundum, orthoclase, albite and hypersthene and distinctly lower in normative anorthite and dioposide than the latter.

4.1.6. Cryptocrystalline chondrule and brown-colored grain

Minute cryptocrystalline chondrules, 0.05 to 0.2 mm in diameter, are dispers-

Table 9. Chemical composition and CIPW norm of cryptocrystalline chondrules and brown-colored grains in the Yamato (a) meteorite (wt. %).

Sample No.	Cryptocrystalline chondrule				Brown-colored grain	
	YA 1	YA 10	YA 11	YA 19	YA 9	YA 31
SiO_2	57.26	55.23	53.52	55.09	51.36	53.26
TiO_2	0.07	0.04	0.01	0.06	0.09	0.19
Al_2O_3	0.03	0.06	0.10	0.03	0.19	1.73
FeO	1.53	2.38	2.15	2.00	1.46	0.98
MnO	0.16	0.29	0.01	0.53	0.00	0.06
MgO	41.10	42.27	44.20	42.43	46.95	41.57
CaO	0.03	0.06	0.21	0.03	0.14	2.97
Na_2O	0.29	0.19	0.15	0.30	0.13	0.22
K_2O	0.03	0.01	0.02	0.02	0.02	0.01
Total	100.50	100.53	100.35	100.49	100.34	100.98
Norm						
Ab	—	—	0.52	—	1.05	2.10
An	—	—	—	—	—	3.62
Ns	0.61	0.37	0.12	0.61	—	—
Di Wo	0.12	0.12	0.46	0.12	0.35	4.65
Di En	0.10	0.10	0.40	0.10	0.30	4.02
Di Fs	—	—	—	—	—	—
Hy En	83.62	72.28	52.34	71.84	48.79	50.50
Hy Fs	2.38	3.30	2.38	2.90	0.92	0.79
Ol Fo	13.09	23.07	33.20	23.92	47.55	34.33
Ol Fa	0.41	1.22	0.85	1.22	1.22	0.61
Il	0.15	—	—	0.15	0.15	0.30
Total	100.48	100.47	100.27	100.50	100.33	100.92

edly embedded in the matrix (Fig. 6). They are pale brown to dark brown in color. They show a smooth and homogeneous appearance under the open nicols. It is observed under the crossed nicols that they are formed of cryptocrystalline materials with strong undulatory extinction. There are several grains, 0.05 to 0.5 mm in size, with the same color and cryptocrystallinity as the above-described chondrules. Some of them have a radial fibrous structure partly in their bodies. Cryptocrystalline chondrules and brown-colored grains have common features in their chemical compositions, that is, both of them are composed mainly of SiO_2 and MgO, being rich in normative hypersthene and olivine (Table 9). The result suggests that they are quenched materials from a liquid which is approximately composed of the orthopyroxene-olivine system, and that they will crystallize olivine and pyroxene grains, if the recrystallization progresses further.

4.1.7. Nickel-iron

Kamacite, α-nickel-iron, is predominant in the opaque phase of the Yamato (a) meteorite. It is identified by its fairly high hardness, isotropic property and light bluish gray color in the reflected light. The grains, from less than 0.001 mm up to 0.5 mm in size, are generally xenomorphic, filling the interstices among the silicate grains in the matrix and chondrules. The intimate intergrowth with troilite, schreibersite and (Mg, Fe, Mn, Ca, Cr)S is common. Troilite and schreibersite are often found as rounded inclusions in kamacite. Perryite, $(Ni, Fe)_x(Si, P)_y$, is also often found in various forms, tabular, platy, worm-like and so on. Rarely minute graphite inclusions are seen. It has been known that kamacite generally intergrows with taenite, γ-nickel-iron, in meteorites, but taenite could not be found in the present section of the Yamato (a) meteorite. Kamacite droplets, less than 0.001 to 0.003 mm in size, are found included in (Mg, Fe, Mn, Ca, Cr)S grains. Another feature of kamacite droplets is found in contact with the myrmekitic intergrowth of troilite and kamacite. In the eccentrically radiating chondrules, minute nickel-iron grains are dispersedly present in the interstices among the alternate pyroxene layers. Kamacite of the Yamato (a) meteorite was found to contain a small amount of silicon by the qualitative X-ray microanalysis. This is an unusual feature of the enstatite chondrite that has not been observed in other meteorite types except the enstatite achondrite (RINGWOOD, 1960; KEIL, 1968).

4.1.8. Troilite

Troilite, FeS, is an abundant opaque mineral next to metallic nickel-iron. It is commonly present in xenomorphic grains, 0.5 mm in maximum size, in intimate contact with metallic nickel-iron, schreibersite and other sulfide minerals. It is identified by its rather dark brown color with strong anisotropism. In the polarized reflected light, it is observed that several troilite grains are intimate aggregates of differently oriented individuals. Troilite frequently includes minute rounded or irregular grains of phosphide or other sulfide minerals. The exsolution lamellae, less than 0.001 mm in width, are notable in the Yamato (a) meteorite (Fig. 17). The exsolved mineral is daubreelite, showing complete isotropism

and greenish-tinged color in the reflected light. Myrmekitic intergrowth with kamacite is present in the form of irregular veins, filling the interstices of silicate phase (Fig. 15). Troilite droplets are present with nickel-iron droplets in the fused silicate veins in the vicinity of the myrmekitic intergrowth (Fig. 16).

4.1.9. (Mg, Fe, Mn, Ca, Cr)S

This mineral is gray in color, completely isotropic and semitransparent in the reflected light. According to the qualitative X-ray microanalysis, this mineral is composed of magnesium, iron and manganese sulfide with small amounts of calcium and chromium. X-ray powder pattern showed that the mineral has a cubic lattice with NaCl structure, and that the cell dimension is about 5.18 Å. This mineral is identified as niningerite, since the optical property and the occurrence are in close agreement with the description of niningerite by KEIL and SNETSINGER (1967) and RAMDOHR (1973). In the Yamato (a) meteorite, the mineral is present in xenomorphic grains, micron-size to 0.2 mm in size, in close contact with kamacite, troilite and schreibersite (Fig. 27). Minute droplets of metallic nickel-iron are frequently included in some grains (Fig. 28). Niningerite has been found only in less extensively recrystallized enstatite chondrites (KEIL, 1968). Ca-rich sulfide mineral is frequently observed in contact with niningerite by the X-ray microanalysis. This is probably oldhamite.

4.1.10. Daubreelite

Daubreelite, $FeCr_2S_4$, is a common mineral in the enstatite chondrite. Minute xenomorphic grains with a greenish tinge, 0.002 to 0.05 mm in size, are found generally in contact with troilite. Fine exsolution lamellae in troilite are common as shown in Fig. 17.

4.1.11. Graphite

Graphite, fairly common mineral in enstatite chondrite, is found in a small amount in the Yamato (a) meteorite. The grains, 0.01 to 0.04 mm in size, are present in aggregates included or in contact with kamacite (Fig. 29). Well-oriented lamellar structure can be seen partly in the graphite aggregate.

4.1.12. Schreibersite

Schreibersite, $(Fe, Ni)_3P$, is present in small grains, micron-size up to 0.1mm in size, in intimate contact with kamacite. It shows a light pinkish tint and weak anisotropism when immersed in oil. It is commonly present at the margin of the kamacite grain, and sometimes it is observed as rounded inclusions in kamacite.

4.1.13. Other accessory minerals

Characteristic X-ray immages of Niα, FeKα, SiKα and PKα showed that Fe-, Si- and P-bearing, nickel-rich grains, 0.01 to 0.05 mm in size, are included in the kamacite grains (Fig. 30). The mineral is tabular, platy and worm-like in shape, and highly reflective. It is identified as perryite, judging from its qualitative X-ray microanalysis and its occurrence (FREDRIKSSON and HENDERSON, 1965; REED, 1968; KEIL, 1968). Fe-bearing zinc sulfide mineral was also found by the qualita-

tive X-ray microanalysis. The mineral, about 0.1 mm in size, isotropic and gray in color, is present in a xenomorphic grain in contact with kamacite, troilite and niningerite. It is probably sphalerite that is often found in enstatite chondrite (RAMDOHR, 1973).

4.2. Yamato (b) meteorite

The Yamato (b) meteorite is a stony meteorite, olive-yellow in color, and its surface is covered with a thin lustrous black crust. The texture of the meteorite is best described as uniformly granular and coarse-grained one (Fig. 31). The minerals are homogeneously distributed throughout the entire mass. The significant feature is that this meteorite is non-chondritic and nearly monomineralic, composed of orthopyroxene. Accessory minerals are clinopyroxene, tridymite, plagioclase, glass, metallic nickel-iron, troilite and chromite. Table 10 shows the modal composition of the Yamato (b) meteorite. Tridymite, plagioclase and chromite are present in xenomorphic grains filling the interstices among the compact assemblage of angular orthopyroxene (bronzite). Chromite is sometimes found as large rounded grains. Devitrified glass, pale brown in color, is rarely found associated with the aggregate of tridymite (Fig. 32). The Yamato (b) meteorite has distinctly achondritic properties showing that it is crystallized like the terrestrial pyroxenite and that it lacks chondrules characteristic of chondritic stony meteorites. According to PRIOR's (1920) classification, this meteorite belongs to the calcium-poor achondrite (SHIMA, SHIMA and HINTENBERGER, 1973; SHIMA, 1974). Hypersthene achondrites as well as enstatite achondrites usually have a brecciated structure with large, angular pyroxene grains occurring in the matrix composed of crushed and broken pyroxene fragments (MASON, 1963). However, the Yamato (b) meteorite is composed of nearly equigranular assemblage of orthopyroxene.

Table 10. Modal composition of the Yamato (b) meteorite (vol. %).

Orthopyroxene	93.0
Clinopyroxene	0.4
Plagioclase	0.1
Tridymite	0.7
Glass	trace
Opaque minerals	5.8
Total	100.0

4.2.1. Orthopyroxene

More than 90 vol. % of the mass is composed of coarse-grained orthopyroxene. The grains, 0.1 to 0.2 mm in size, are almost colorless, without pleochroism. The optical properties and unit cell parameters of orthopyroxene are as follows:

Optic axial angle : 2V (aver.)$=-70°$
Refractive index : $\alpha_D=1.682$, $\beta_D=1.691$-1.694, $\gamma_D=1.698$
Pleochroism : None

Unit cell paramenters: $a=18.274\pm0.002$Å
$b=8.874\pm0.001$Å
$c=5.203\pm0.001$Å

Chemical composition of orthopyroxene is shown in Table 11. The average molar composition is $En_{75}Fs_{25}$, indicating bronzite. Therefore the Yamato (b) meteorite belongs to the so-called "hypersthene achondrite" of PRIOR (1920), which is actually composed of bronzite. The molar composition of orthopyroxene of the hypersthene achondrite is remarkably uniform, $En_{75}Fs_{25}$ to $En_{73}Fs_{27}$ (average: $En_{74}Fs_{26}$) (MASON, 1963). In comparison with the analytical data of orthopyroxene

Table 11. Chemical composition of orthopyroxene in the Yamato (b) meteorite (wt. %).

Sample No.	SiO_2	TiO_2	Al_2O_3	FeO	MnO	MgO	CaO	Na_2O	K_2O	Total
YB 1	54.44	0.12	1.03	15.86	0.49	26.03	1.42	0.01	0.01	99.42
YB 3	55.43	0.06	0.47	15.28	0.59	27.03	0.97	0.02	0.01	99.85
YB 4	55.62	0.03	0.44	15.59	0.57	26.92	0.95	0.01	0.02	100.15
YB 5	54.83	0.06	0.43	15.62	0.52	27.46	0.95	0.00	0.01	99.88
YB 6	55.15	0.02	0.44	15.11	0.51	27.12	0.94	0.01	0.00	99.29
YB 8	55.07	0.10	0.90	15.94	0.51	26.66	1.35	0.01	0.00	100.54
YB 10	54.48	0.02	0.70	15.93	0.50	26.65	1.15	0.01	0.00	99.43
YB 11	55.40	0.01	0.42	15.74	0.48	26.71	0.98	0.00	0.00	99.73
YB 12	54.75	0.07	1.13	15.52	0.50	25.88	1.37	0.05	0.00	99.28
YB 13	54.43	0.12	1.27	15.73	0.53	26.01	1.44	0.05	0.00	99.59
Average	54.96	0.06	0.72	15.63	0.52	26.65	1.15	0.02	0.01	99.72

Average structural formula :
$(Ca_{0.046}\ Na_{0.001})\ (Mg_{1.437}\ Fe_{0.474}\ Ti_{0.002}\ Mn_{0.015}\ Al_{0.019})\ (Si_{1.989}\ Al_{0.011})O_6$

of the Johnstown and Tatahouine hypersthene achondrites (MASON, 1963), the orthopyroxene of the Yamato (b) meteorite is much lower in TiO_2 and Na_2O contents. MASON (1963) observed the exsolution lamellae of clinopyroxene (probably diopside) in orthopyroxene of the Johnstown, Ibbenbuhren, Manegaon and Roda hypersthene achondrites, indicating that the pyroxene primarily crystallized at temperatures higher than the diopside-hypersthene solvus. However the clinopyroxene exsolution lamellae are not observed in the orthopyroxene of the Yamato (b) meteorite. Orthopyroxene grains have numerous opaque inclusions, fine-grained up to 0.05 mm in size. Fluid inclusions, 0.02 mm in maximum size, are also dispersedly present in spheroidal, ovoid, ellipsoidal, teardrop-like and irregularly elongated forms (Fig. 33).

4.2.2. Clinopyroxene

Minor amount of clinopyroxene, 0.1 to 0.4 mm in size, is present surrounded by orthopyroxene grains. It is nonpleochroic and optically positive. The extinction angle ($c\wedge Z$) is 40°-42°, and the optic orientation is $Y=b$. Suitable

grains for the determination of the optic axial angle were not found in the thin section. The exsolution lamellae of orthopyroxene, about 0.001 mm in width, are present along the (100) partings of the clinopyroxene (Fig. 34). The lamellar orthopyroxene (bronzite) and the host clinopyroxene share the (100) plane and b-axis with each other (Fig. 35).

4.2.3. Plagioclase

Small grains of twinned plagioclase, less than 0.02mm in size, are present as shown in Fig. 36. The refractive index is $\alpha_D=1.564$ and $\gamma_D=1.572$, indicating $Ab_{31}An_{69}$ in molar composition.

4.2.4. Tridymite

Tridymite in hypersthene achondrite was reported only in the Ibbenbuhren meteorite (TSCHERMAK, 1885), but the occurrence was doubted by MASON (1963) later. Though small in amount, tridymite is fairly common in the Yamato (b) meteorite. It is present in xenomorphic grains filling the interstices among orthopyroxene, opaque minerals and devitrified glass (Fig. 32). The average optic axial angle is +65°, and the refractive index is $\alpha_D=1.479$ and $\gamma_D=1.483$. The wedge-shaped, interpenetration twinning is common. The pseudohexagonal twinning frequently seen in aragonite is also found, in which a- and b-axes of the individual sets of the twin are at angle of 60° with each other, sharing the common c-axis. Table 12 shows the electron microprobe data of tridymite.

Table 12. Chemical composition of tridymite in the Yamato (b) meteorite (wt. %).

Sample No.	SiO_2	TiO_2	Al_2O_3	FeO	MnO	MgO	CaO	Na_2O	K_2O	Total
YB 2	98.94	0.10	0.73	0.17	0.01	0.02	0.16	0.19	0.02	100.34

4.2.5 Chromite

Chromite, $FeCr_2O_4$, is a major component of the opaque phase in the Yamato (b) meteorite. It is 0.5 to 1.5 mm in size in the matrix, and is slightly translucent in the very thin section or finely crushed grains, showing a reddish brown color. The grains are weakly magnetic, and show X-ray powder pattern of spinel-type.

4.2.6. Other accessory minerals

Xenomorphic grains of troilite and metallic nickel-iron are present in a small amount as interstitially filling material among orthopyroxene grains. However, most of troilite and nickel-iron grains are dispersed in the form of finely droplet-like inclusions in pyroxene grains.

4.3. Yamato (c) meteorite

The Yamato (c) meteorite is friable and strongly magnetic. It shows dull black color owing to the dispersive occurrence of fine opaque grains in the mass. The meteorite generally consists of fine-grained mass with chondritic structure (Fig. 37). It is composed mainly of olivine and opaque minerals, with small amounts of plagioclase, pyroxene and spinel-like grains. Table 13 shows the

Table 13. Modal composition of the Yamato (c) meteorite (vol. %).

Matrix	Orthopyroxene	1.3
	Clinopyroxene	0.8
	Olivine	63.5
	Plagioclase	11.5
	Opaque minerals	22.9
Total		100.0
Chondrule	Olivine	88.9
	Plagioclase	1.7
	Opaque minerals	9.4
Total		100.0
Matrix		94.5
Chondrule		5.5
Total		100.0

modal composition of the Yamato (c) meteorite. The opaque mineral phase is composed of magnetite and pentlandite with a small amount of troilite. Metallic nickel-iron is extremely low in content. Chondrules are all spheroidal in shape, and they are 0.2 to 0.8 mm in diameter, occupying about 5 vol. % of the mass. Most of them are granular type, and are composed of congregated olivine grains, 0.002 to 0.1 mm in size, and a small amount of spherular opaque grains (Fig. 38). A barred-type chondrule which is composed of alternate olivine layers interstitially filled with plagioclase and dark material is also found. The monomineralic chondrules composed of large olivine grains, 0.1 to 0.7 mm in size, are most notable (Fig. 39). A chondrule shown in Fig. 40 has a characteristic structure. It is surrounded by an outer crust formed of olivine, while the inner part is composed of rod-like olivine crystals interstitially filled with dark material. There are spheroidal opaque grains consisting of complex aggregate of magnetite, pentlandite and troilite (Fig. 41). Fig. 42 shows an interesting feature of a chondrule, as if one olivine chondrule and one opaque chondrule were encountered with each other. The matrix, about 95 vol. % of the entire mass, is dominated by fine-grained olivine and plagioclase and finely dispersed opaque grains. However, larger olivine grains, 0.08 to 0.5 mm in size and euhedral to subhedral in shape, also coexist in the fine-grained matrix. The opaque minerals are present in such various forms as fine grains, spherules, nodules, veins and their combined structures. Magnetite, pentlandite and troilite generally occur in contact with one another, forming aggregates filling the interstices among silicate grains. Plagioclase is present in xenomorphic grains, including numerous opaque grains and spinel-like mineral, 0.001 to 0.01 mm in size and greenish in color (Fig. 43). Minute cubic grains in the interstitial plagioclase are assumed to be magnetite

and spinel-like mineral. In addition, thin needles of pyroxene are also included in plagioclase as shown in Fig. 44. Fig. 45 shows a cataclastically sheared structure of orthopyroxene grain, as if it has been subjected to violent stress. The Yamato (c) meteorite has several characteristics of carbonaceous chondrite, that is, a friable and dark-colored mass, the presence of magnetite and nearly absent metallic nickel-iron. Under the microscope, amorphous hydrated silicates, serpentine or chlorite which are characteristic of the type I or type II carbonaceous chondrite could not be found in the thin section. The main mass of the Yamato (c) meteorite is mostly made up of olivine, indicating that this meteorite corresponds to the type III carbonaceous chondrite (MASON, 1962b). The result is in agreement with the conclusion from the chemistry of the Yamato (c) meteorite by SHIMA, SHIMA and HINTENBERGER (1973) and SHIMA (1974).

4.3.1. Olivine

Olivine is a dominant constituent of the Yamato (c) meteorite, and is colorless to slightly brown in color. Its size is up to 0.7 mm in maximum, but mostly less than 0.01 mm. Zonal structure is frequently observed. In the transmitted light, it looks pale brown in the core and very pale brown in the margin, and show weak pleochroism, that is X: slightly pale brown, Z: very pale brown (X>Z). Fine opaque inclusions are commonly present, especially along the fractures in crystals.

In addition to opaque inclusions, some olivine grains include minute rod-like grains, greenish brown in color, 0.005 to 0.02 mm in length and about 0.002 mm in width (Fig. 46). Pleochroism: Z′, greenish brown, X′, pale greenish brown (Z′>X′); Elongation: positive; Extinction angle: $c \wedge Z = 14°-15°$; Birefringence: low. Refractive index is much lower than that of olivine. These inclusions are present in parallel to or slightly inclined to the c-axis of olivine, but their identification was not possible.

Table 14. Chemical composition of olivine in the Yamato (c) miteorite (wt. %).

Sample No.	SiO_2	TiO_2	Al_2O_3	FeO	MnO	MgO	CaO	Na_2O	K_2O	Total	Note
YC 2	38.09	0.02	0.02	26.46	0.23	35.32	0.01	0.01	0.01	100.17	Matrix
YC 7	38.21	0.04	0.05	26.63	0.23	34.97	0.02	0.00	0.01	100.15	Matrix
YC 9	37.77	0.09	0.02	26.72	0.21	35.02	0.03	0.00	0.00	99.86	Chondrule
YC 10	38.10	0.04	0.04	26.97	0.25	34.45	0.10	0.06	0.01	100.01	Matrix
YC 13	37.64	0.11	0.08	27.14	0.19	34.55	0.01	0.03	0.01	99.76	Matrix
YC 15	37.75	0.00	0.06	26.67	0.22	34.72	0.04	0.01	0.01	99.48	Matrix
YC 17	38.34	0.00	0.05	27.01	0.29	35.14	0.03	0.01	0.00	100.88	Chondrule
YC 20	38.28	0.00	0.04	26.04	0.24	35.57	0.02	0.01	0.01	100.21	Chondrule
YC 25	38.54	0.00	0.12	26.25	0.23	34.82	0.03	0.00	0.01	100.00	Matrix
Average	38.08	0.03	0.05	26.65	0.23	34.95	0.03	0.01	0.01	100.06	

Average structural formula:

$(Ca_{0.002}\ Na_{0.001})\ (Mg_{1.381}\ Fe_{0.591}\ Ti_{0.001}\ Mn_{0.005}\ Al_{0.002})\ Si_{1.010}O_4$

The optical properties and unit cell parameters of olivine are as follows:
Optic axial angle: 2V (aver.)= −85° for the matrix olivine.
−86° for the olivine in chondrules.
Refractive index: α_D=1.683, γ_D=1.725
Unit cell parameters: a=4.783±0.008 Å
b=10.244±0.009 Å
c=6.008±0.004 Å

Table 14 shows the electron probe data of olivine in the Yamato (c) meteorite. The average composition of olivine shows $Fo_{70}Fa_{30}$ in molar composition. In the type III carbonaceous chondrites, it is known that the chemical composition of olivine is very variable from grain to grain in a single meteorite. For example, the olivine in the Grosnaja and Mokoia meteorites ranges from zero to 60 mole percent Fe_2SiO_4 (MASON, 1962b), and that of the Allende meteorite from zero to 45 mole percent Fe_2SiO_4 (CLARKE *et al.*, 1970). Therefore, it is better to calculate the average composition of olivine from its d_{130} spacing in the X-ray powder pattern of the Yamato (c) meteorite, which gives $Fo_{80}Fa_{20}$ in mole percent from the determinative curve by YODER and SAHAMA (1957).

4.3.2. Pyroxene

Pyroxene is rare in chondrules, and it occurs mainly in the matrix, although in a small amount. Orthopyroxene is pale yellow in color, and shows very weak pleochroism; X: very pale brown, Z: very pale yellow (X>Z). The optic axial angle (2V) is −66°. Clinopyroxene is present associated with orthopyroxene along the (100) partings of the latter. The extinction angle (c∧Z) is about 42°. Thin needle-like orthopyroxene and clinopyroxene crystals are also included in plagioclase. They are colorless to pale yellow, and are generally 0.02 to 0.1 mm in length and less than 0.002 mm in width (Fig. 49). Polysynthetic twinning is frequently found in larger grains of clinopyroxene. The extinction angles (c∧Z) are 41°-42°. The electron probe data of orthopyroxene shows that its composition is $En_{73}Fs_{27}$ (Table 15).

Table 15. Chemical composition of orthopyroxene in the Yamato (c) meteorite (wt. %).

Sample No.	SiO_2	TiO_2	Al_2O_3	FeO	MnO	MgO	CaO	Na_2O	K_2O	Total	Note
YC 11	54.33	0.01	1.52	16.60	0.18	26.30	0.35	0.00	0.00	99.30	Matrix
YC 12	53.47	0.00	2.48	17.17	0.22	25.54	0.28	0.02	0.00	99.19	Matrix
YC 28	54.93	0.00	1.46	16.63	0.27	26.74	0.32	0.01	0.00	100.36	Matrix
Average	54.24	0.00	1.82	16.80	0.22	26.19	0.32	0.01	0.00	99.62	

Average structural formula:
$(Ca_{0.013}\ Na_{0.001})\ (Mg_{1.417}\ Fe_{0.510}\ Mn_{0.007}\ Al_{0.046})\ (Si_{1.968}\ Al_{0.032})O_6$

4.3.3. Plagioclase

Plagioclase is present in xenomorphic grains filling the interstices among the silicate and opaque mineral grains, and shows strong undulatory extinction.

Table 16. Chemieal composition of plagioclase in the Yamato (c) meteorite (wt. %).

Sample No.	SiO_2	TiO_2	Al_2O_3	FeO	MnO	MgO	CaO	Na_2O	K_2O	Total	Note
YC 4	43.57	0.04	34.66	0.64	0.00	0.04	19.83	0.39	0.01	99.18	Chondrule
YC 5	54.05	0.00	28.08	0.19	0.00	0.03	12.11	4.92	0.17	99.56	Chondrule
YC 8	61.28	0.00	24.05	0.25	0.00	0.01	6.57	8.64	0.63	101.45	Matrix
YC 14	61.75	0.00	23.87	0.15	0.00	0.01	6.20	8.96	0.20	101.56	Matrix

Structural formula

YC 4: $(Ca_{3.982}\ Na_{0.141}\ K_{0.002})\ (Mg_{0.012}\ Fe_{0.100}\ Ti_{0.006}\ Al_{5.826})\ (Si_{8.167}\ Al_{1.833})O_{32}$

YC 5: $(Ca_{2.362}\ Na_{1.737}\ K_{0.039})\ (Mg_{0.008}\ Fe_{0.030}\ Al_{5.862})\ (Si_{9.837}\ Al_{0.163})O_{32}$

YC 8: $(Ca_{1.244}\ Na_{2.958}\ K_{0.142})\ (Mg_{0.004}\ Fe_{0.038}\ Al_{5.009})\ Si_{10.825}O_{32}$

YCl 4: $(Ca_{1.170}\ Na_{3.063}\ K_{0.139})\ (Mg_{0.004}\ Fe_{0.022}\ Al_{4.960})\ Si_{10.882}O_{32}$

Twinning is common, mostly albite-type and rarely Carlsbad-type. The grain size and shape of plagioclase vary from grain to grain because of xenomorphic intergrowth of plagioclase with olivine and opaque minerals. In chondrules, plagioclase occurs as minute grains filling the interstices among olivine grains. The optical properties of plagioclase grains in the matrix are as follows:

Optic axial angle: 2V (aver.)$=+86°$

Refractive index: $\alpha_D=1.551$, $\gamma_D=1.560$

Plagioclase corresponds to high-temperature andesine ($Ab_{55}An_{45}$) (SMITH, 1958). However, the electron probe data of four plagioclase grains suggest that the chemical composition is different from grain to grain (Table 16), ranging from oligoclase ($Or_3Ab_{68}An_{29}$) to anorthite (Ab_3An_{97}). It is assumed that this fact is due to the unequilibrated characteristic of the Yamato (c) meteorite. In addition to pyroxene inclusions as shown in Fig. 44, minute magnetite grains are commonly present in plagioclase. Fine spinel-like grains, greenish in color, are also found with magnetite in plagioclase.

4.3.3. Magnetite

Magnetite is notably found in the opaque phase of the Yamato (c) meteorite, and the strongly magnetic property of this meteorite is due to the abundance of magnetite, which is in agreement with the nature of the type III carbonaceous chondrite. Magnetite occurs as rounded or xenomorphic grains, ranging from less than 0.001 to 0.2 mm in size, and sometimes as short veins. Generally it coexists with sulfide minerals, pentlandite and troilite. Minute magnetite grains in plagioclase are euhedral, less than 0.001 to 0.02 mm in size (Fig. 43). Exsolution lamellae of ilmenite, less than 0.002 mm in width, occur in some grains of magnetite (Fig. 47). The lattice constant of magnetite is $a=8.397\pm0.003$ Å, which was calculated from d_{800}, d_{731} and d_{444} spacings of the Debye-Scherrer photograph taken under the Mn-filtered Fe Kα radiation, using silicon as an internal standard.

4.3.4. Ilmenite

Ilmenite, $FeTiO_3$, has been found in most of olivine-bronzite and olivine-hypersthene chondrites. Among the carbonaceous chondrites, Cold Bokkeveld

(type II) contains this mineral (RAMDOHR, 1973). In the Yamato (c) meteorite, the exsolution lamellae of ilmenite, less than 0.002 mm in width, are found in magnetite, probably parallel to the octahedral plane of magnetite. Ilmenite is dark brown in color, much darker than magnetite, and it is distinguishable by its strong anisotropism and distinct reflection pleochroism.

4.3.5. Pentlandite, troilite and nickel-iron

Pentlandite, $(Ni, Fe)_9S_8$, is not rare in carbonaceous chondrite (MASON, 1962b). The type III carbonaceous ones, Allende, Grosnaja, Kaba and Mokoia, contain this mineral according to RAMDOHR (1973). Pentlandite, predominant in the sulfide phase of the Yamato (c) meteorite, occurs as both independent and xenomorphic grains, less than 0.1 mm in size. It has a light creamy color and isotropic property. Single grains of pentlandite take idiomorphic forms with well-developed cleavages (Fig. 48). Pentlandite generally coexists with magnetite or troilite. The intergrowth of pentlandite and patches of troilite, less than 0.005 mm in size, is common, as shown in Fig. 49. Very minute patches of nickel-iron are rarely found.

4.4. Yamato (d) meteorite

The Yamato (d) meteorite is an olivine-bronzite chondrite. It is composed mainly of olivine, orthopyroxene (bronzite) and opaque minerals with small amounts of plagioclase and clinopyroxene (Table 17). The opaque phase of the meteorite consists of kamacite, taenite, troilite, chromite and metallic copper.

Table 17. Modal composition of the Yamato (d) meteorite (vol. %).

Matrix	Orthopyroxene	31.7
	Clinopyroxene	0.8
	Olivine	41.4
	Plagioclase	9.8
	Spinel-like mineral	trace
	Opaque minerals	16.3
Total		100.0
Chondrule	Olivine	84.2
	Plagioclase	15.8
Total		100.0
Matrix		99.2
Chondrule		0.8
Total		100.0

Part of metallic nickel-iron and troilite grains are locally oxidized by the terrestrial weathering, as shown by the local staining of iron oxide. The Yamato (d) meteorite has a chondritic structure, though it is poorly found in the section.

Chondrules composed of alternate layers of olivine interstitially filled with plagioclase are present in the crystalline mass. They are generally spheroidal in shape, ranging from 0.2 to 0.5 mm in diameter. Their boundaries are fairly indefinable because of the intergrowth between matrix and chondrules (Fig. 50). The matrix is composed of compact assemblage of well-crystallized olivine and pyroxene grains interstitially filled with xenomorphic plagioclase grains. Olivine and orthopyroxene are distinctly angular, and coarse grains of olivine and orthopyroxene in euhedral and subhedral forms are present associated with finely crushed angular fragments of olivine and orthopyroxene. Opaque minerals, metallic nickel-iron, troilite and chromite, generally occur as coarse grains, and sometimes as xenomorphic grains or veins interstitially filling among the silicate grains in the matrix. Fine droplets of metallic nickel-iron and troilite, less than 0.002 mm in diameter, are locally present in clusters near the large nickel-iron and troilite grains (Fig. 51). Such occurrence is frequently found in stony meteorites (FISH *et al.*, 1960; RAMDOHR, 1963, 1973). RAMDOHR (1973) suggested the possibility of fusions by local breaking.

4.4.1. Olivine

Olivine is a dominant silicate mineral of the Yamato (d) meteorite, and occupies the most part of the matrix and chondrules. The grains, 0.3 mm in maximum size, are mostly angular and rich in irregular fractures. Most of them show wavy extinction. Some grains are surrounded by the needles of orthopyroxene. The optical properties and unit cell parameters of olivine are as follows:

Optic axial angle: 2V (aver.)$=-88°$ for the matrix olivine.
Refractive index: $\alpha_D=1.666$, $\gamma_D=1.709$
Unit cell parameters: a$=4.763\pm0.001$ Å
b$=10.249\pm0.001$ Å
c$=6.005\pm0.001$ Å

The average molar composition of olivine is $Fo_{82}Fa_{18}$. Fig. 52 shows a recrystallized olivine, which is disintegrated into fine aggregates of olivine crystals, 0.005 to 0.01 mm in size, retaining the original euhedral form. According to CARTER *et al.* (1968), such a structure of olivine is due to the deformation by shock effect.

4.4.2. Pyroxene

Orthopyroxene is a dominant silicate mineral next to olivine. It is colorless and its size ranges up to 0.3 mm. The grains are angular, and (110) cleavages and (100) partings are well-developed. Orthopyroxene is locally concentrated in the entire mass, forming aggregates. The optical properties and unit cell parameters of orthopyroxene are as follows:

Optic axial angle: 2V (aver.)$=-88°$
Refractive index: $\alpha_D=1.671$, $\gamma_D=1.686$
Pleochroism: None
Unit cell parameters: a$=18.268\pm0.009$ Å
b$=8.850\pm0.005$ Å

$$c = 5.202 \pm 0.002\ \text{Å}$$

Average molar composition of orthopyroxene is $En_{84}Fs_{16}$. Some grains of orthopyroxene are surrounded by thin reaction rim of augite ($c \wedge Z = 40°$-$45°$). Augite and host orthopyroxene share b-axis and (100) plane with each other as shown in Fig. 53.

4.4.3. Plagioclase

Plagioclase is present in xenomorphic grains filling the interstices among olivine and pyroxene grains. In chondrules, plagioclase coexists with olivine, interstitially filling the alternate layers of olivine. The optical properties of plagioclase are as follows:

Optic axial angle: 2V (aver.) $= -61°$ for the matrix plagioclase.
$-62°$ for the plagioclase in chondrules.

Refractive index: $\alpha_D = 1.535$, $\gamma_D = 1.546$

Molar composition is Ab_{79}-Ab_{78}, indicating high-temperature oligoclase. Polysynthetic twinning on albite law is common. Plagioclase includes minute droplet-like inclusions of olivine and pyroxene along the grain boundaries with olivine and pyroxene (Fig. 54). Droplets show spheroidal, ellipsoidal, ovoid and teardrop-like forms, as if they were once melted.

4.4.4. Spinel-like mineral

Fine grains of spinel-like mineral, 0.002 to 0.02 mm in size, are dispersedly included in plagioclase, olivine and orthopyroxene grains. They are isotropic, red to reddish brown in color, and idiomorphic in shape (Fig. 55).

4.4.5. Nickel-iron

Metallic nickel-irons, kamacite and taenite, are very common in the olivine-bronzite chondrites. They occur as coarse grains, 0.5 mm in maximum size, sometimes as xenomorphic veins among silicate grains, or in intimate contact with troilite and chromite (Fig. 56). Kamacite, α-nickel-iron, is more abundant than taenite, γ-nickel-iron. Although both nickel-irons are isotropic, kamacite shows a light bluish gray color, and taenite is creamy white in color. Both minerals usually occur in intimate contact with each other (Fig. 57).

4.4.6. Copper

Single phase of native copper occurs in small grains in most stony meteorites (RAMDOHR, 1963, 1973; KEIL and FREDRIKSSON, 1963; DUKE and BRETT, 1965). A minute grain of copper, about 0.005 mm in size, was found associated with troilite and kamacite in the Yamato (d) meteorite (Fig. 58). Copper shows a pink color with high reflectivity, but soon tarnishes into a brown color. The electron microprobe studies showed that meteoritic copper was not pure, containing a considerable amount of iron, 1-4.5 wt. % (KEIL and FREDRIKSSON, 1963; DUKE and BRETT, 1965).

4.4.7. Troilite

Troilite, one of the predominant mineral species of the opaque phase in the Yamato (d) meteorite, is generally found as coarse grains, 0.02 mm in maximum

size, or as short veins being xenomorphic among silicate grains. Intergrowth with metallic nickel-iron and chromite is common. Under the crossed nicols in the reflected light, it is found that the troilite grain is an aggregate of differently oriented crystals.

4.4.8. Chromite

Chromite occurs as fairly large grains, 0.1 mm in maximum size. Xenomorphic grains in intimate contact with metallic nickel-iron and troilite, and independent rounded grains are also common.

4.5. Yamato (g) meteorite

The Yamato (g) meteorite is a stony meteorite with a chondritic structure (Fig. 59). Its major mineral constituents are olivine, orthopyroxene (bronzite), clinopyroxene, plagioclase and opaque minerals (Table 18). In the silicate phase, olivine is predominant, and orthopyroxene comes next. Coarse grains of olivine and orthopyroxene, and chondrules are dispersedly embedded in the granular matrix composed mainly of olivine and pyroxene grains. The opaque minerals are dispersed in xenomorphic grains, less than 0.001 to 0.8 mm in size, throughout the matrix, filling the interstices among silicate grains. Narrow veinlets of opaque minerals are also present penetrating the matrix and branching along the boundaries of silicate grains and chondrules. In some cases, the veins cut single silicate grains and chondrules, indicating that the intrusion of opaque veins took place

Table 18. Modal composition of the Yamato (g) meteorite (vol. %).

Matrix	Orthopyroxene	13.0
	Clinopyroxene	0.2
	Olivine	61.0
	Plagioclase	2.3
	Opaque minerals	22.3
	Others*	1.2
Total		100.0
Chondrule	Orthopyroxene	23.6
	Clinopyroxene	1.1
	Olivine	71.0
	Plagioclase	1.1
	Opaque minerals	3.2
Total		100.0
Matrix		93.6
Chondrule		6.4
Total		100.0

* Brown-colored oxidation products of terrestrial weathering of metallic and sulfide minerals.

after the agglomeration of silicate phase. Some of the opaque grains are oxidized into reddish brown iron oxide minerals which locally stain the silicate grains pale brownish yellow. Chondrules, 0.1 to 1.5 mm in size, are common in this meteorite, and they are composed mainly of olivine and orthopyroxene with minor amounts of clinopyroxene, plagioclase and opaque grains. Glass is not present. Most chondrules are irregularly deformed, while spheroidal ones are rare. Various structural types of chondrules are seen in the Yamato (g) meteorite, that is, the granular type, the eccentrically radiating type, the barred-type, and so on. Fig. 60 shows a typically granular chondrule composed of euhedral and subhedral grains of olivine. A chondrule monosomatically composed of larger olivine grains takes a conglomelated form. An eccentrically radiating form of chondrule is seen in Fig. 61. This chondrule is formed of fibrous orthopyroxene crystals. Fig. 62 shows another fibrous type of chondrule consisting of fibrous crystals of olivine interstitially filled with clinopyroxene. This chondrule is distinctly deformed and has a complicated layer structure. Barred chondrules formed of olivine or orthopyroxene layers are also common (Fig. 63). The interstices between the layers are generally filled with plagioclase and dark material, but no interstitial glass is found. The interstices among the phenocrysts in chondrules are, however, frequently filled with micron-size silicate grains and finely fibrous materials which were probably derived from the recrystallization of the interstitial glass. The boundaries of chondrules are generally less distinct owing to the intergrowth between chondrules and matrix.

4.5.1. Olivine

The grains range from micron-size up to 0.8 mm in size. Most grains in the matrix are fragmental and subhedral in shape. Euhedral grains are found only in the granular chondrules. Under the crossed nicols, most of olivine grains show distinctly wavy extinction, and sometimes kink bands. Corroded grains and pyroxene-rimmed ones are frequently found in the matrix. The optical property of olivine is as follows:

Optic axial angle: 2V (aver.)$=-87°$ for the matrix olivine.
$-87°$ for the olivine in chondrules.

The average molar composition is $Fo_{79}Fa_{21}$ for both the matrix olivine and the olivine in chondrules.

4.5.2. Pyroxene

Fragmental orthopyroxene grains, 0.4 mm in maximum size, are most common in this meteorite. Euhedral and subhedral grains are found in the microporphyritic chondrules. The optical properties of orthopyroxene are as follows:

Optic axial angle: 2V (aver.)$=-82°$ for the matrix orthopyroxene.
$-81°$ for the orthopyroxene in chondrules.

Pleochroism: None

Average molar composition of orthopyroxene is $En_{80}Fs_{20}$. Several orthopyroxene grains in both the matrix and chondrules are partly surrounded by the reaction rim of augite ($c \wedge Z = 35°$), (100) plane and b-axis of which are common to those

of orthopyroxene. Some grains of augite surrounding orthopyroxene as a reaction rim have exsolution lamellae of clinopyroxene as seen in Fig. 64. Optical orientation and extinction angle of the exsolved clinopyroxene are $X=b$ and $c \wedge Z = 29°$. Host augite and lamellar clinopyroxene are common in (001) plane and b-axis to each other (Fig. 65). Fig. 66 shows an orthopyroxene grain bearing a kink band associated with lamellar clinopyroxene.

4.5.3. Plagioclase

A small amount of plagioclase occurs as xenomorphic grains, less than 0.1mm in size, in the interstices among the fragmental olivine and pyroxene grains. In the barred-type chondrules, plagioclase fills the interstices among the alternate layers of olivine. Albite-twinned plagioclase is common. The optical properties of plagioclase in the matrix are as follows:

Optic axial angle: $2V$ (aver.)$= +88°$

Refractive index: $\alpha_D = 1.535$, $\gamma_D = 1.544$

Plagioclase in this meteorite is $Ab_{85}An_{15}$ in average molar composition, and has low-temperature structural state.

4.5.4. Opaque minerals

Opaque grains are present in xenomorphic forms among the silicate grains and chondrules. Opaque phase is also present in veins linking with xenomorphic opaque grains and branching thin veinlets in network through the silicate phase. Kamacite and taenite were identified by the X-ray powder pattern of metallic grains separated from the pulverized sample. Fig. 67 shows the occurrence of opaque droplets dispersing along the dark, partially fused silicate veins.

Acknowledgments

The author wishes to express his hearty thanks to Prof. K. Yagi of the Hokkaido University, for his great interest and guidance in this work, and to Dr. Makoto Shima of the Institute of Physical and Chemical Research, for his continuous support and guidance throughout the work. The author is greatly indebted to Dr. K. Onuma, Dr. Y. Hariya and Mr. S. Terada of the Hokkaido University, for their kind suggestions in the optical and X-ray works on meteorites, and to Prof. M. Hunahashi and Dr. T. Tsuchiya of the Hokkaido University, for their valuable advices for the identification of opaque minerals. The specimens were obtained from the collection of the meteorites at the Tokyo University of Education through the courtesy of Prof. M. Gorai of the University. The bulk chemical data of the Yamato meteorites were kindly supplied by Dr. Masako Shima, McMaster University. Drs. S. Igi, T. Soya and K. Okumura of the Geological Survey of Japan kindly provided the author with the opportunity of the electron probe microanalyses of minerals. The author is especially indebted to Mr. H. Yabuki and Mrs. S. Yabuki of the Institute of Physical and Chemical Research, for their generous support during the course of the work. The author wishes to thank all these persons.

References

ALLEN, R. O. and B. MASON (1973): Minor and trace elements in some meteoritic minerals. Geochim. Cosmochim. Acta, **37**, 1435–1456.

ANDERS, E. (1964): Origin, age and composition of meteorites. Space Sci. Rev., **3**, 583–714.

BINNS, R. A. (1967): Olivine in enstatite chondrites. Am. Mineral., **52**, 1549–1554.

CARTER, N. L., C. B. RALEIGH, and P. S. DECARLI (1968): Deformation of olivine in stony meteorites. J. Geophys. Res., **73**, 5439–5461.

CLARKE, R. S., E. JAROSEWICH, B. MASON, J. NELEN, M. GOMEZ, and J. R. HYDE (1970): The Allende, Mexico, meteorite shower. Smithonian Contrib. Earth Sci., **5**, 1–53.

DUKE, M. B. and R. BRETT (1965): Metallic copper in stony meteorites. U. S. Geol. Survey Profess. Papers, **525-B**, B 101.

FISH, R. A., G. G. GOLES and E. ANDERS (1960): The record in meteorites, III. On the development of meteorites in asteroidal bodies. Astrophys. J., **132**, 243–258.

FREDRIKSSON, K. and E. P. HENDERSON (1965): The Horse Creek, Baca County, Colorado, iron meteorite. Trans. Am. Geophys. Union, **46**, 121.

HEY, M. H. (1966): Catalogue of Meteorites, 3rd. Ed., 637 pp., British Museum, London.

HOWIE, R. A. (1963): Mineral. Soc. Am. Special Paper, No. 1.

JAHANBAGLOO, I. C. (1969): X-ray diffraction study of olivine solid solution series. Am. Mineral., **54**, 246–250.

KAWACHI, Y. (1971): Calculation of mineral formula for EPMA analysis. Geology-1051.

KEIL, K. (1968): Mineralogical and chemical relationships among enstatite chondrites. J. Geophys. Res., **73**, 6945-6976.

KEIL, K. and K. FREDRIKSSON (1963): Electron microprobe analysis of some rare minerals in the Norton County achondrite. Geochim. Cosmochim. Acta, **27**, 939-947.

KEIL, K. and G. SNETSINGER (1967): Niningerite: a new meteoritic sulfide. Science, **155**, 451–453.

KUNO, H. (1954): Study of orthopyroxenes from volcanic rocks. Am. Mineral., **39**, 30–46.

MASON, B. (1962a): Meteorites, 274 pp., Wiley, New York.

MASON, B. (1962b): The carbonaceous chondrites. Space Sci. Rev., **1**, 621-646.

MASON, B. (1963): The hypersthene achondrites. Am. Mus. Novitates, **2155**, 13 pp.

MASON, B. (1966): The enstatite chondrites. Geochim. Cosmochim. Acta, **30**, 23–39.

NAKATSUKA, T. (1974), Combination of Geology-1010 and Geology-1051, and modification for TOSBAC-340.

OKUMURA, K. and Y. KAWACHI (1971): Correction for EPMA quantitative analysis. Geology-1010.

PRIOR, G. T. (1920): The classification of meteorites. Mineral. Mag., **19**, 51–63.

RAMDOHR, P. (1963): The opaque minerals in stony meteorites. J. Geophys. Res., **68**, 2011–2036.

RAMDOHR, P. (1973): The Opaque Minerals in Stony Meteorites, 245 pp., Akademie-Verlag, Berlin.

REED, S. J. B. (1968): Perryite in the Kota-Kota and South Oman enstatite chondrites. Mineral. Mag., **36**, 850–854.

REID, A. M. and A. J. COHEN (1967): Some characteristics of enstatite from enstatite chondrites. Geochim. Cosmochim. Acta, **31**, 661–672.

REID, A. M. and K. FREDRIKSSON (1967): Chondrules and chondrites. Researches in Geochemistry (Abelson, P. H. ed.), **2**, 170–203, Wiley, New York.

RINGWOOD, A. E. (1960): Silicon in metal phase of enstatite chondrites. Nature, **186**, 465–466.

SHIMA, M. (1966): Glassy spherules (microtektite?) found in ice at Scott Base, Antarctica. J.

Geophys. Res., **71**, 3595–3596.

SHIMA, M. (1970): The study of cosmic dust. Bull. Inst. Space Aeronaut. Sci., **6**, 120–141 (in Japanese).

SHIMA, Masako (1974): The chemical composition of the stone meteorites Yamato (a), (b), (c) and (d) and Numakai. Meteoritics, **9**, 123–135.

SHIMA, Masako, A. OKADA, and M. SHIMA (1973): Study on the extraterrestrial materials at Antarctica (III). Antarct. Rec., **47**, 86–97 (in Japanese).

SHIMA, M., A. OKADA and Masako SHIMA (1974): Study on the extraterrestrial materials at Antarctica (IV). Antarct. Rec., **48**, 91–99 (in Japanese).

SHIMA, M., Masako SHIMA and H. HINTENBERGER (1973): Chemical composition and rare gas content of four new detected Antarctic meteorites. Earth Planet. Sci. Letters, **19**, 246–249.

SHIMA, M. and H. YABUKI (1968): Study on the extraterrestrial materials at Antarctica (I). Antarct. Rec., **33**, 53–64 (in Japanese).

SHIMA, M., H. YABUKI and A. OKADA (1969): Study on the extraterrstrial materials at Antarctica (II). Antarct. Rec., **84**, 1–13 (in Japanese).

SHIMA, M., H. YABUKI, A. OKADA and S. YABUKI (1972): The study of cosmic dust. Space Research XII, 301–308, Akademie-Verlag, Berlin.

SMITH, J. R. (1958): The optical properties of heated plagioclase. Am. Mineral., **43**, 1179–1192.

STEPHENSON, D. A., C. B. SCLAR and J. V. SMITH (1966): Unit cell volumes of synthetic orthoenstatite and low clinoenstatite. Mineral. Mag., **35**, 838–846.

SUWA, K. and K. NAGASAWA (1961): A correction diagram for measuring an inclination angle with the universal stage. J. Earth Sci., **9**, 29.

SWEATMAN, T. R. and J. V. P. LONG (1969): Quantitative electron-probe microanalysis for rock-forming minerals. J. Petrol., **10**, 332–379.

YABUKI, S., A. OKADA, H. YABUKI and M. SHIMA (1969): On the study of cosmic dust (V). Sci. Papers IPCR, **45**, 149–155 (in Japanese).

YODER, H. S. and T. G. SAHAMA (1957): Olivine X-ray determinative curve. Am. Mineral., **49**, 475–491.

YOSHIDA, M., H. ANDO, K. OMOTO, R. NARUSE and Y. AGETA (1971): Discovery of meteorites near Yamato Mountains, East Antarctica. Antarct. Rec., **39**, 62–65.

(*Received May 12, 1975*)

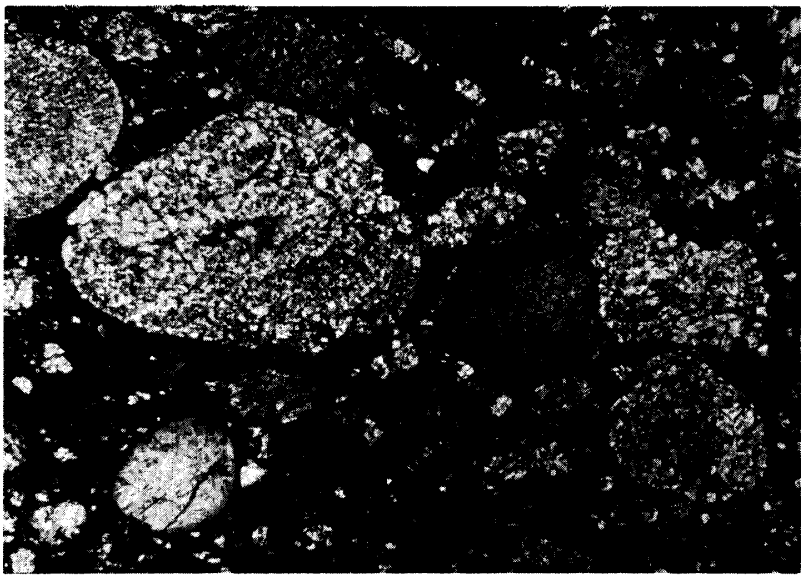

Fig. 3. A thin section of the Yamato (a) meteorite. Chondritic structure is notable. Abundant chondrules and chondrule fragments are seen embedded in the opaque matrix. Transmitted light. ×40.

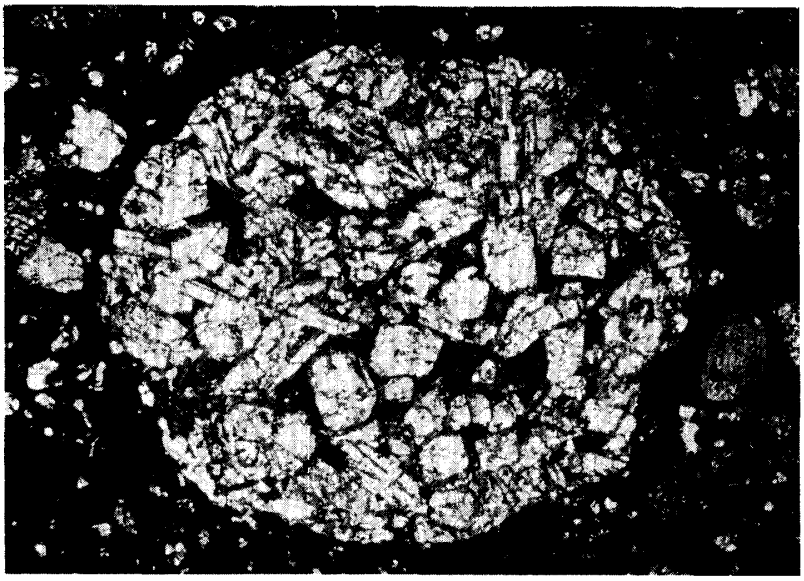

Fig. 4. A granular chondrule with microporphyritic structure consisting of enstatite, clinoenstatite, olivine and devitrified glass. Yamato (a). Transmitted light, ×51.

Fig. 5. A barred chondrule consisting of thin layers of orthopyroxene. Yamato (a). Transmitted light. ×51.

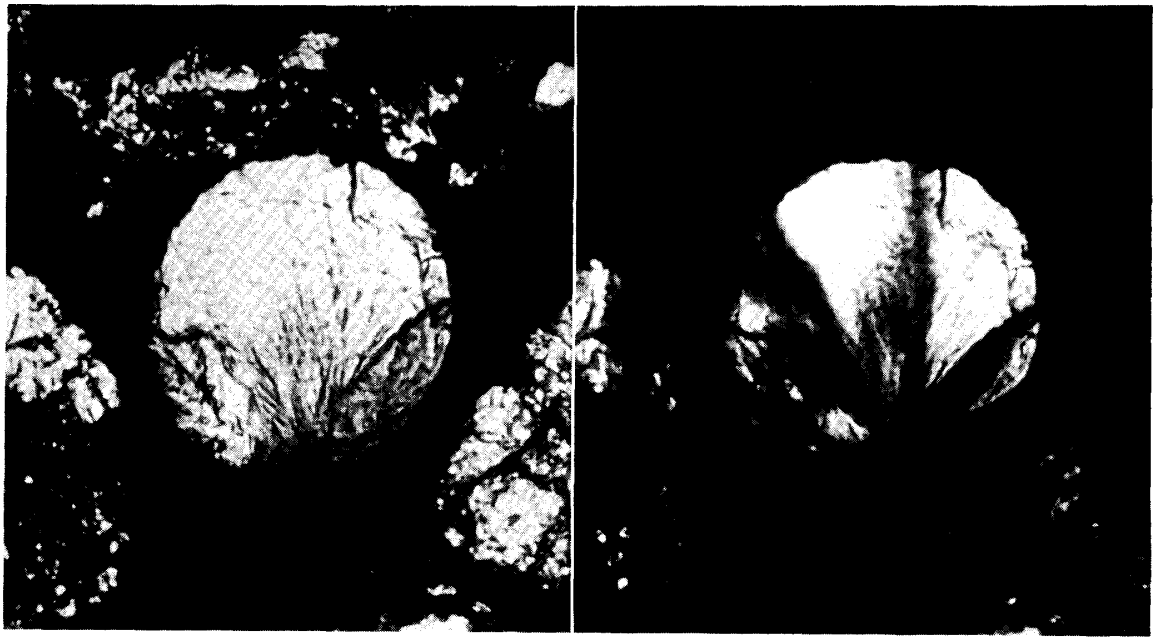

Fig. 6. A cryptocrystalline chondrule. It shows a strongly wavy extinction. Yamato(a). Transmitted light. ×430. Left: Nicol not crossed. Right: Nicol crossed.

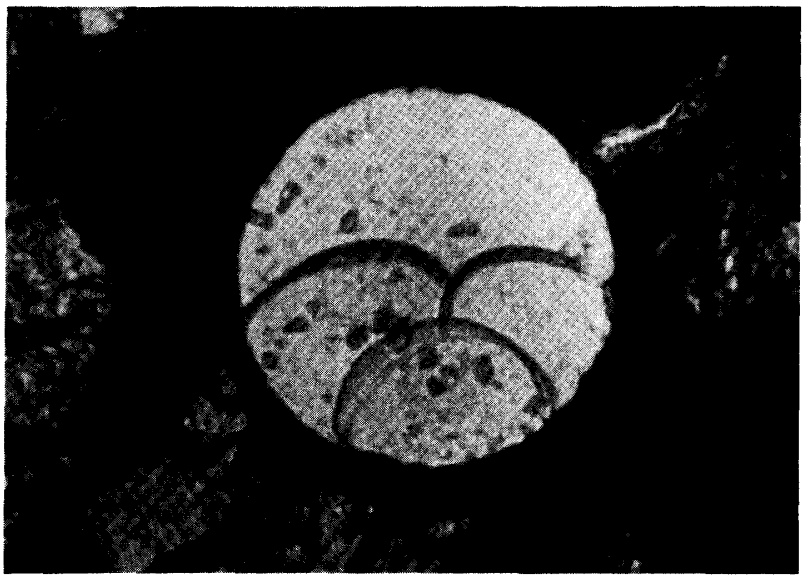

Fig. 7. A spherular form of cristobalite. Yamato (a). Transmitted light. ×220.

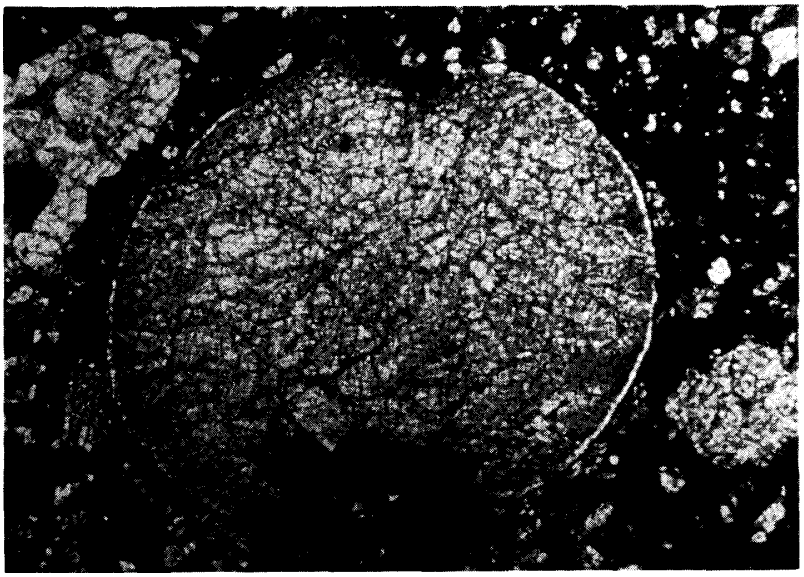

Fig. 8. An enstatite chondrule partly broken in the margin. Yamato (a). Transmitted light. ×46.

Fig. 9. A crescent form of chondrule fragment composed of orthopyroxene. Yamato (a). Transmitted light. ×57.

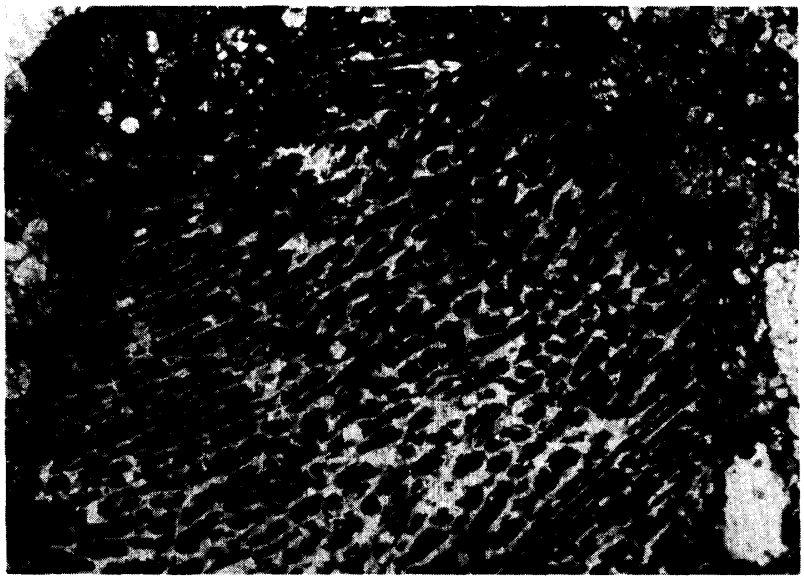

Fig. 10. A metallic nickel-iron chondrule interstitially filled with clinopyroxene and plagioclase. Yamato (a). Transmitted light. ×34.

Fig. 11. A pyroxene chondrule fragment with sheared and folded internal structure. Yamato (a). Transmitted light. ×51.

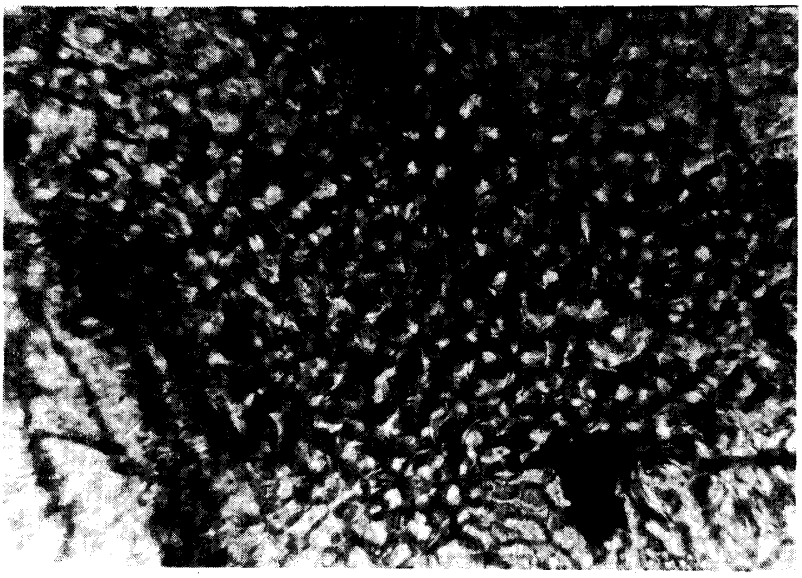

Fig. 12. Droplet-like pyroxene aggregate in the pyroxene chondrule fragment in Fig. 9. Yamato (a). Transmitted light. ×710.

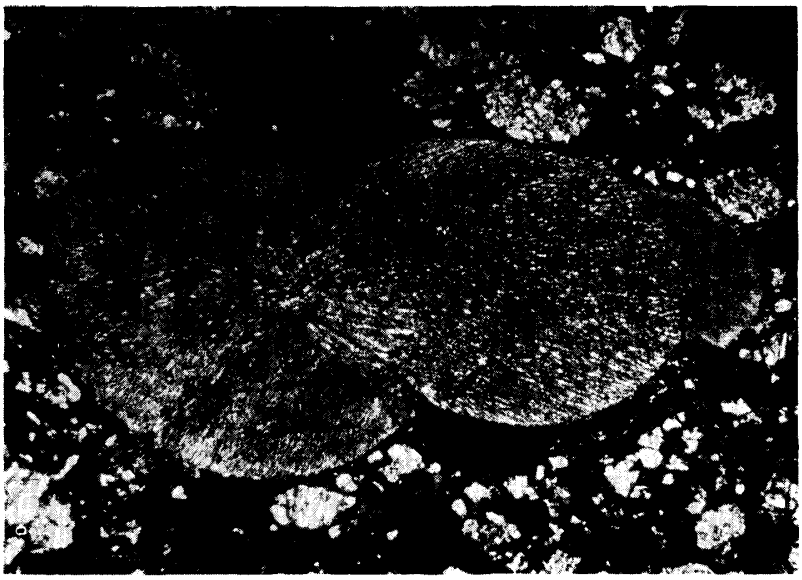

Fig. 13. A manifoldly joined chondrule composed of fibrous orthopyroxene. Yamato (a). Transmitted light. ×10.

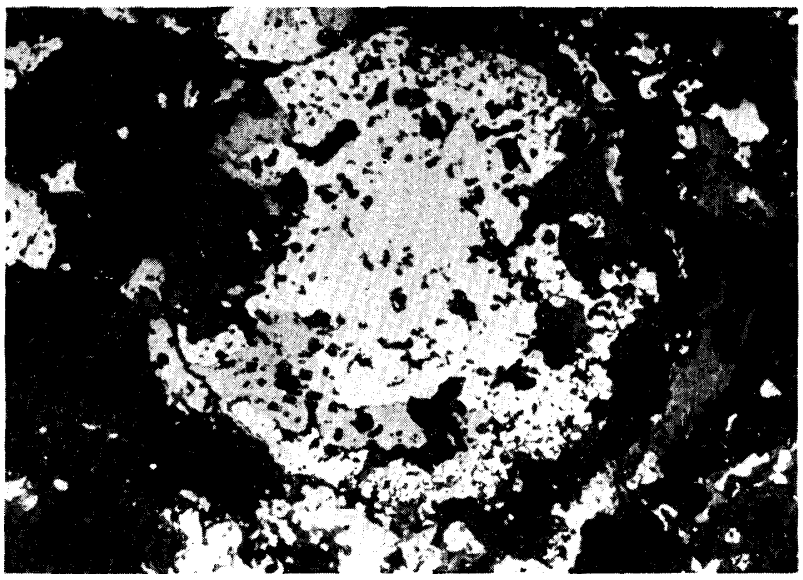

Fig. 14. A chondrule-like aggregate of kamacite (white), troilite (gray), nininger ite (dark gray) and schreibersite. Yamato(a). Reflected light. ×260. In this picture, schreibersite is not distinguishable because of low contrast with kamacite.

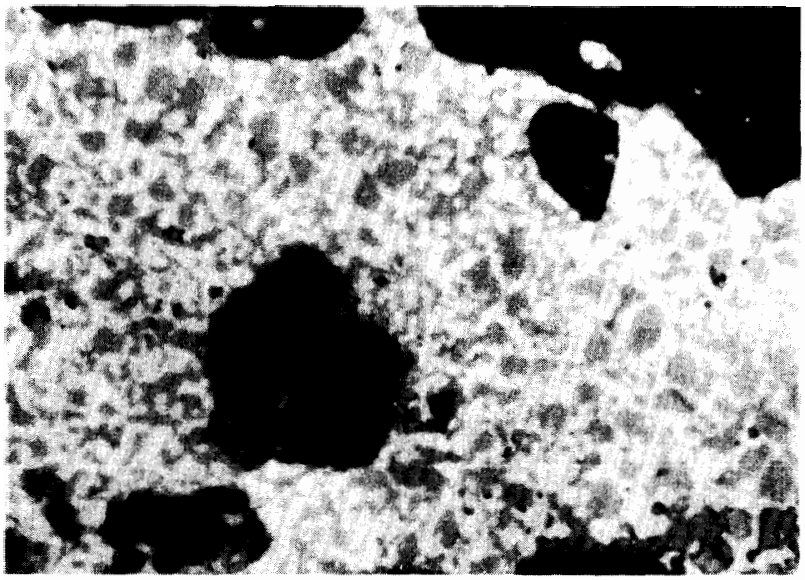

Fig. 15. Myrmekitic intergrowth of nickel-iron (white) and troilite (gray). Yamato (a). Reflected light. ×1800.

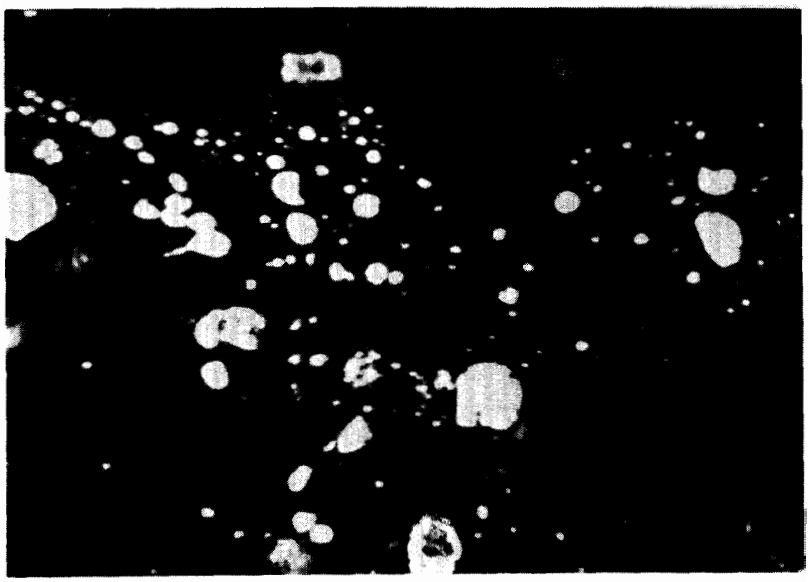

Fig. 16. Fused droplets of nickel-iron and troilite. They occur in the fused veins of silicates near the myrmekitic intergrowth of troilite and nickel-iron. Yamato (a). Reflected light. ×4400.

Fig. 17. Exsolution lamellae of daubreelite (gray) in troilite (light gray) associated with schreibersite (white). Yamato(a). Reflected light. ×1500.

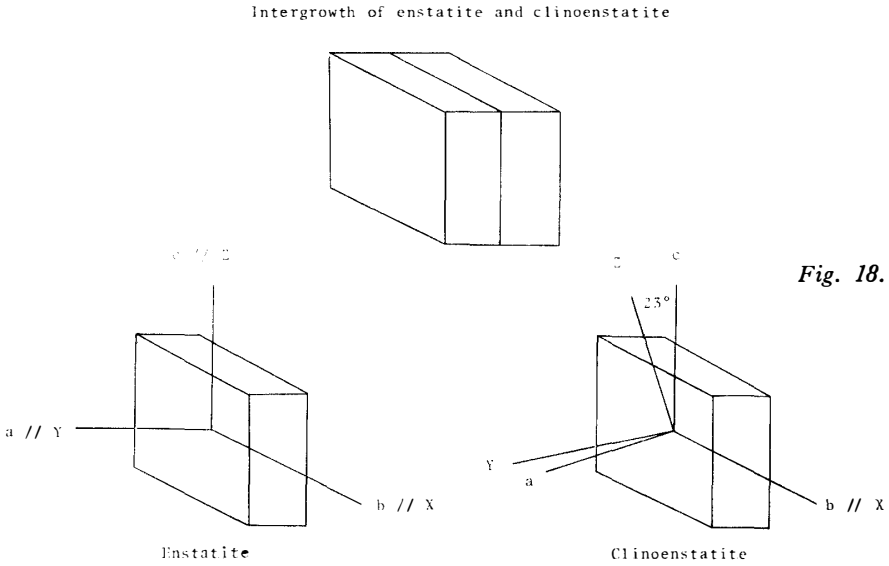

Fig. 18. The arrangement of optical and crystallographic axes of enstatite and clinoenstatite.

Fig. 19. Polysynthetic twinning of clinoenstatite. Yamato (a). Transmitted light. Nicol crossed. ×430.

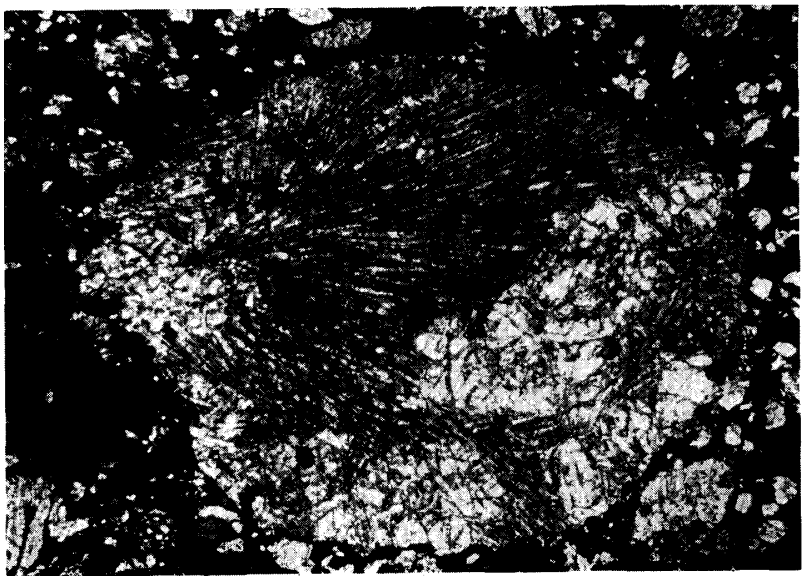

Fig. 20. Olivine grains in the radiating pyroxene chondrule. Olivine is thinly rimmed with orthopyroxene. Yamato (a). Transmitted light. ×18.

Fig. 21. Enstatite-rimmed olivine grain in the matrix. Yamato(a). Transmitted light. ×130.

Fig. 22. Cristobalite grains in the radiating pyroxene chondrule. Yamato (a). Transmitted light. ×63.

Fig. 23. The occurrence of glass and devitrified glass in chondrules. Yamato (a). Transmitted light. Left: Pale brown, transparent glass filling the interstices among enstatite and clinoenstatite grains. ×200. Right: Devitrified glass grading into dark brown, fine material. ×140.

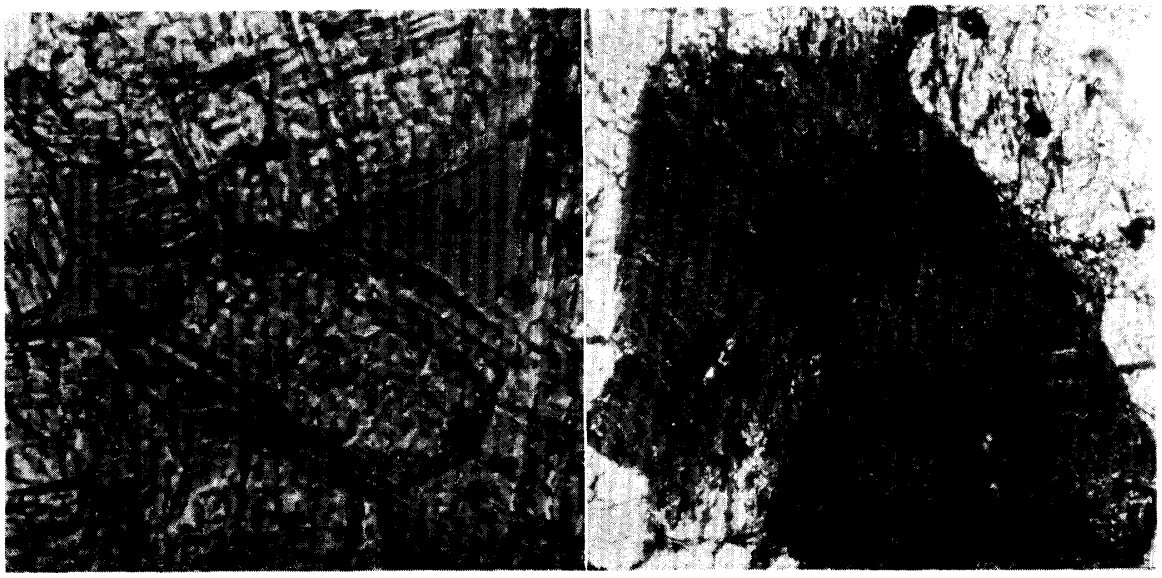

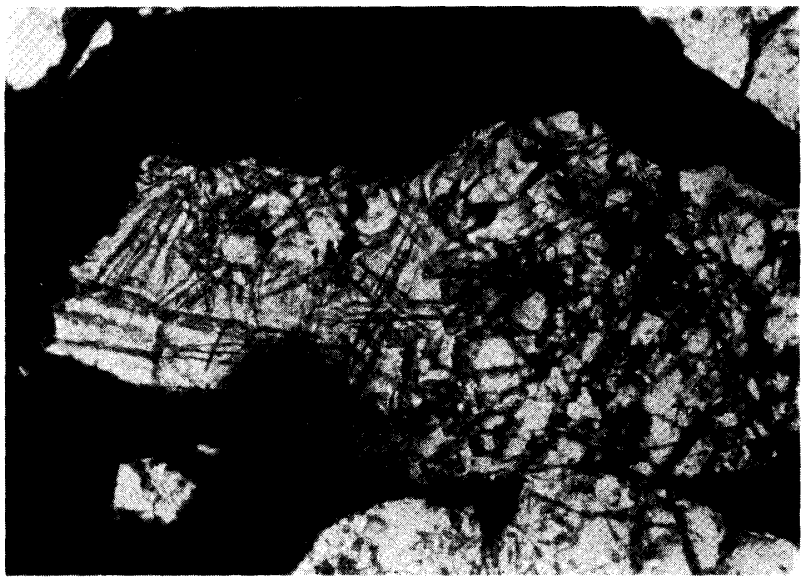

Fig. 24. Pale brown glass bearing thinly crystallized pyroxene. Yamato (a). Transmitted light. ×140.

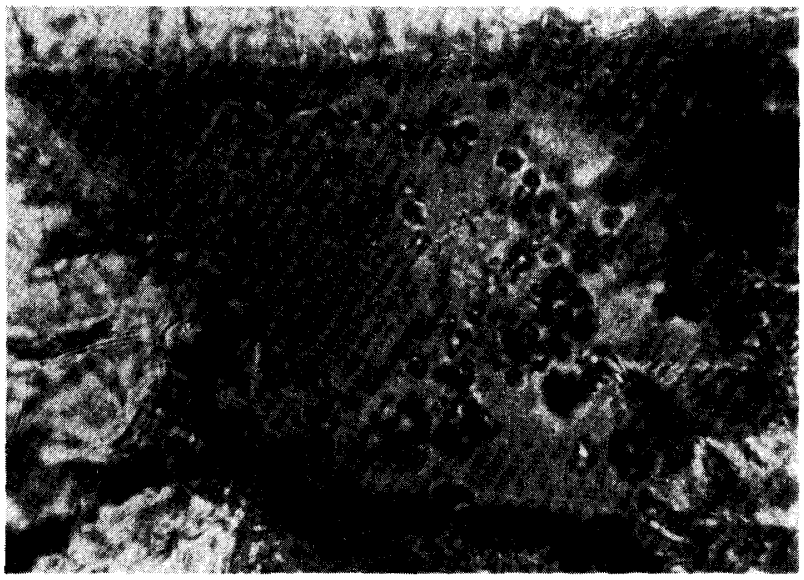

Fig. 25. Spinel-like grains included in the partially devitrified glass. Yamato (a). Transmitted light. ×480.

Fig. 26. Dendritic form of crystallites in the partially devitrified glass. Yamato (a). Transmitted light. ×830.

Fig. 27. Assemblage of opaque minerals, niningerite (dark gray), troilite (gray), nickel-iron and schreibersite (white). Yamato (a). Reflected light. ×480

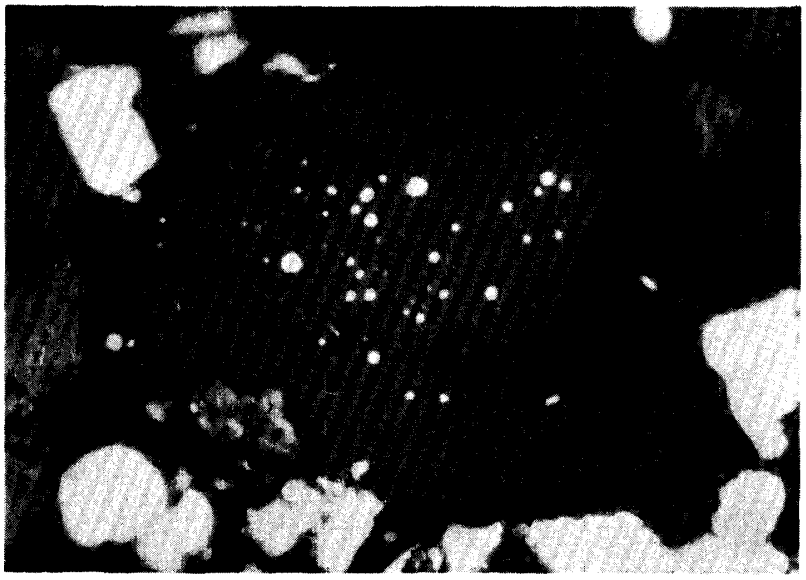

Fig. 28. Niningerite (dark gray) including minute metallic nickel-iron droplets (white). Yamato (a). Reflected light. ×1600.

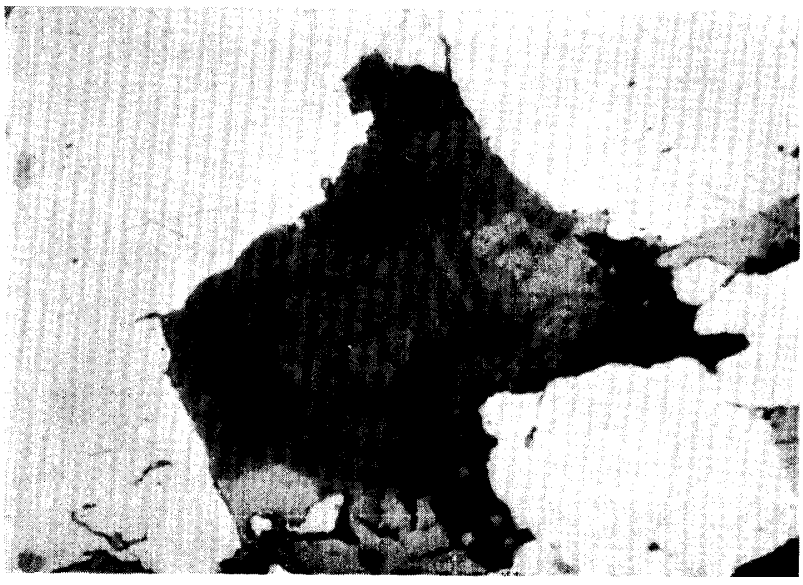

Fig. 29. Graphite aggregate in kamacite grain. Lamellar structure is locally found. Yamato (a). Reflected light. ×570.

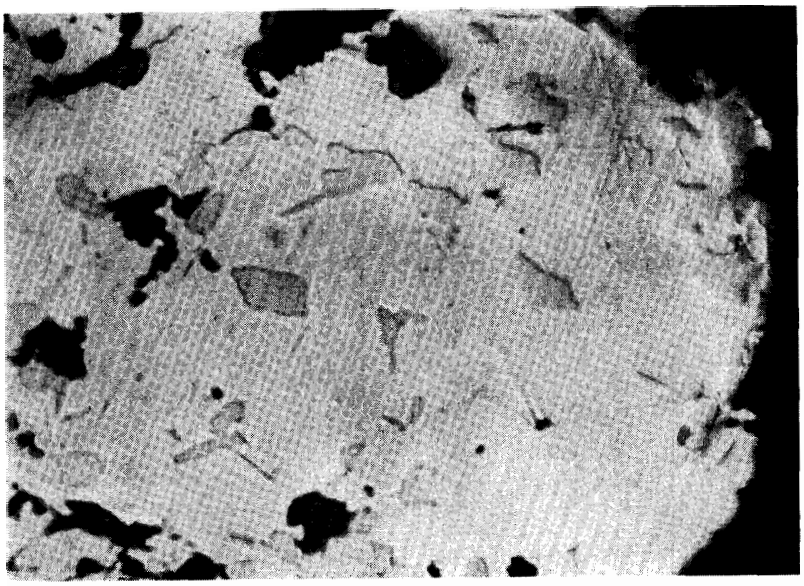

Fig. 30. Perryite occurring included in kamacite. Yamato (a). Reflected light. ×740.

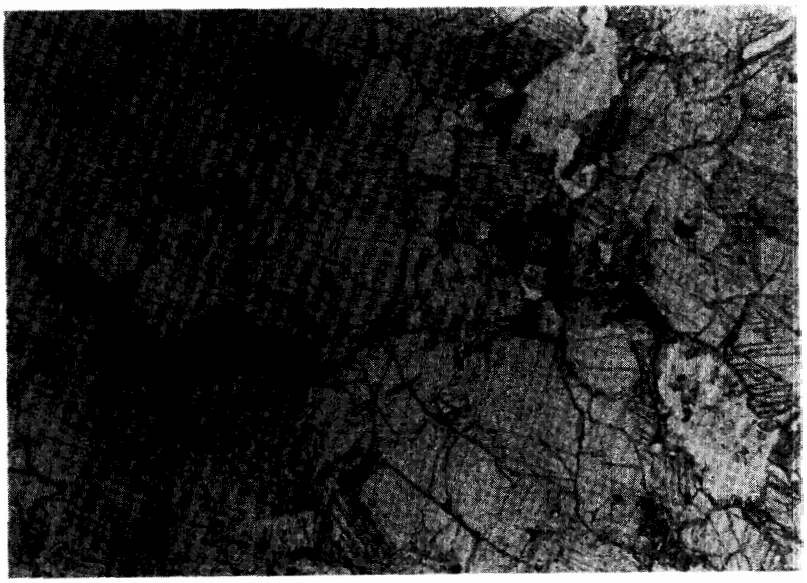

Fig. 31. A thin section of the Yamato (b) meteorite. The entire mass is composed mostly of compact assemblage of bronzite grains. Opaque grains are nickel-iron, troilite and chromite. Transmitted light. ×46.

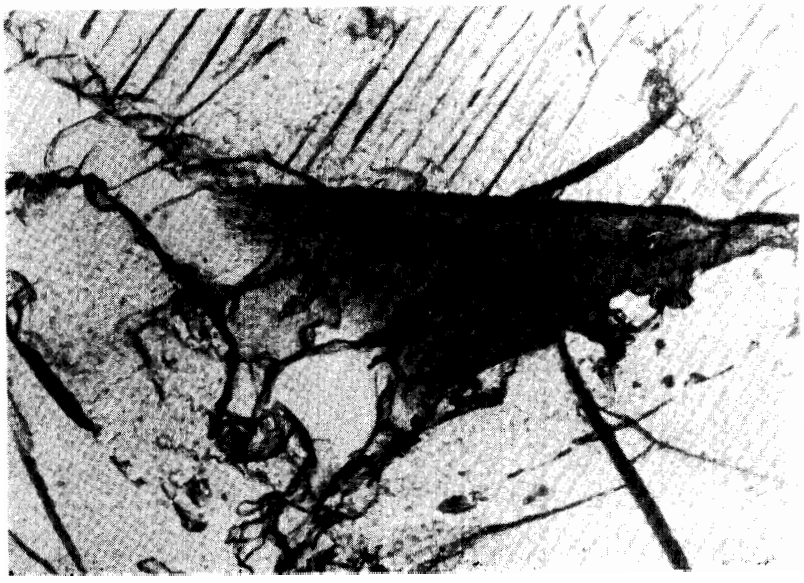

Fig. 32. Pale brown, devitrified glass and tridymite grains filling the interstices among bronzite grains. Yamato (b). Transmitted light. ×320.

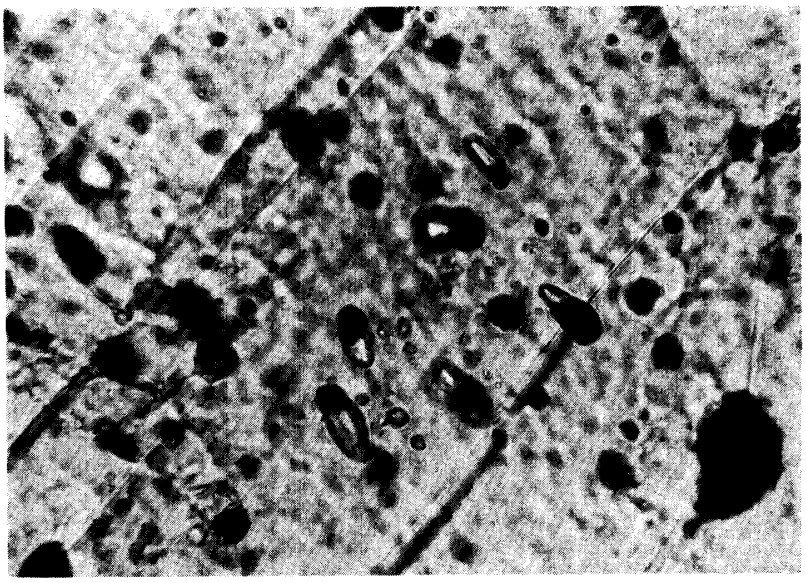

Fig. 33. Opaque and fluid inclusions dispersed in orthopyroxene grains. Opaque grains are generally troilite and nickel-iron. Yamato (b). Transmitted light. ×800.

Fig. 34. Exsolution lamellae of orthopyroxene in clinopyroxene (probably diopside). Yamato (b). Transmitted light. Nicol crossed. ×320.

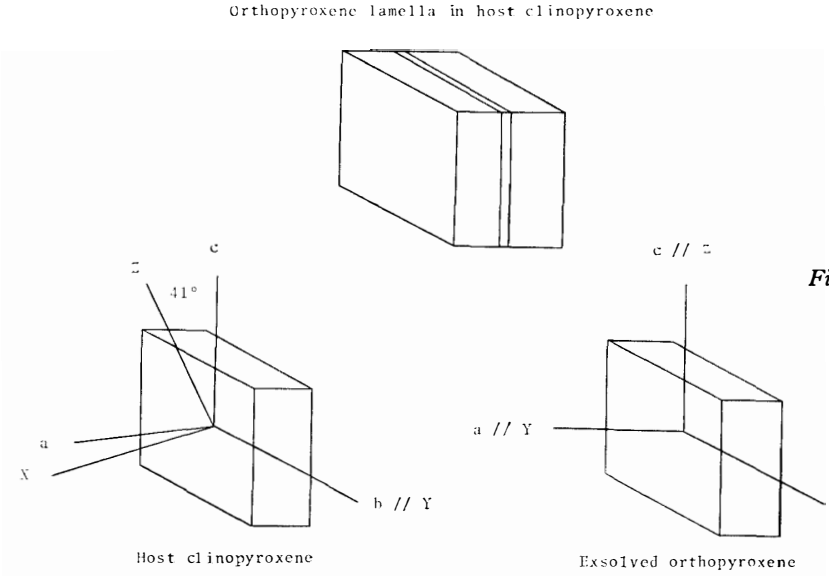

Fig. 35. The arrangement of optical and crystallographic axes of host clinopyroxene and lamellar orthopyroxene.

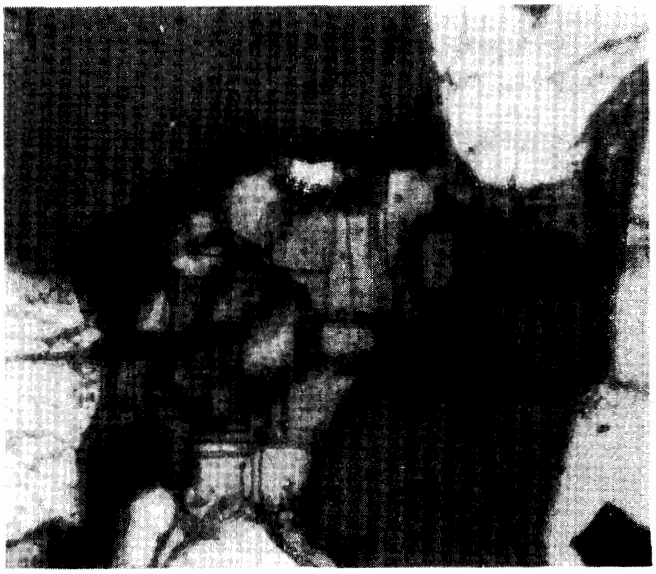

Fig. 36. Twinned plagioclase occurring in the interstice among orthopyroxene grains. Yamato (b). Transmitted light. Nicol crossed, but the stage was rotated 45° from the extinction position for taking photograph. ×330.

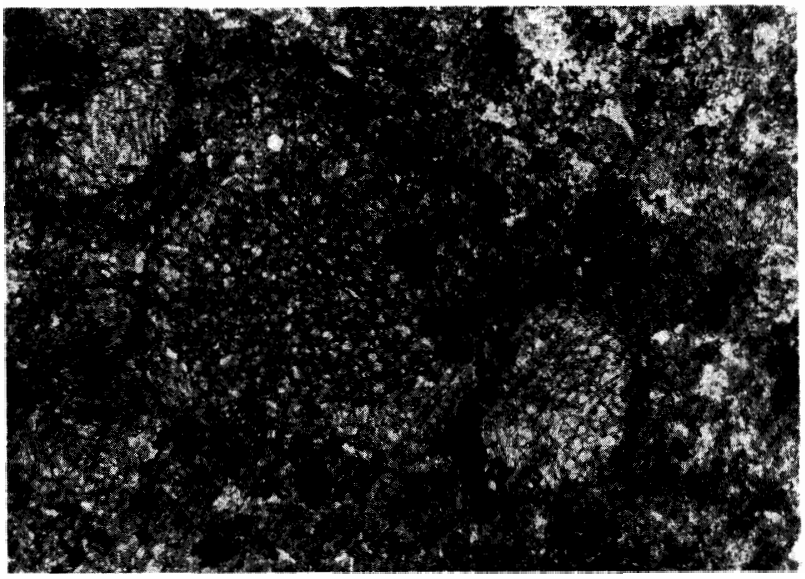

Fig. 37. A thin section of the Yamato (c) meteorite. This meteorite is chondritic, and its dark-colored matrix is composed largely of olivine. Fine grains of magnetite are dispersed throughout the mass. Transmitted light. ×34.

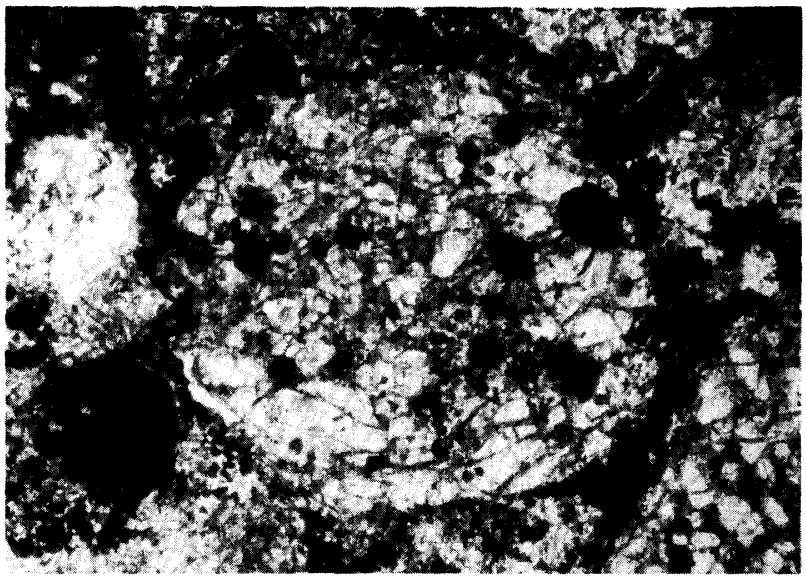

Fig. 38. A granular chondrule made up of small olivine grains. This chondrule includes spheroidal opaque grains, mainly magnetite with accessory amounts of pentlandite and troilite. Yamato(c). Transmitted light. ×110.

Fig. 39. A chondrule composed of larger grains of olivine. Yamato (c). Transmitted light. ×91.

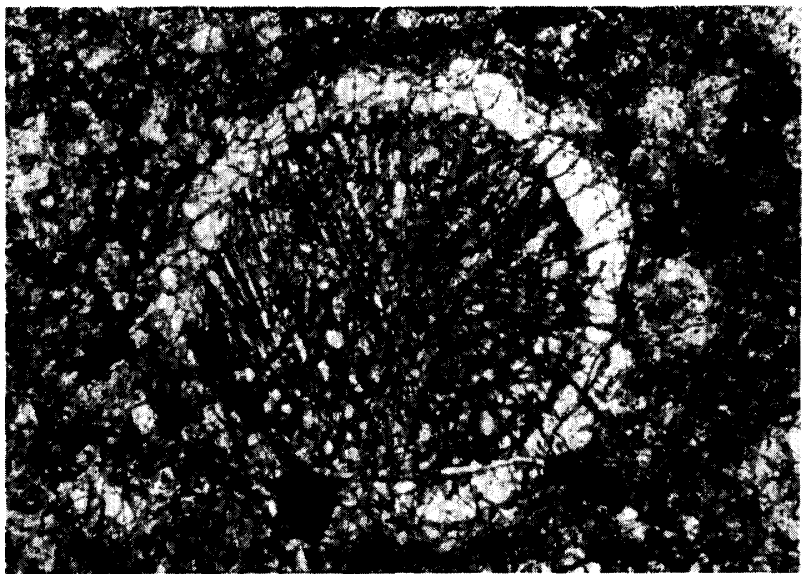

Fig. 40. An olivine chondrule bearing an outer crust in the periphery. The interior is composed of rod-like olivine crystals interstitially filled with dark material. Yamato (c). Transmitted light. ×69.

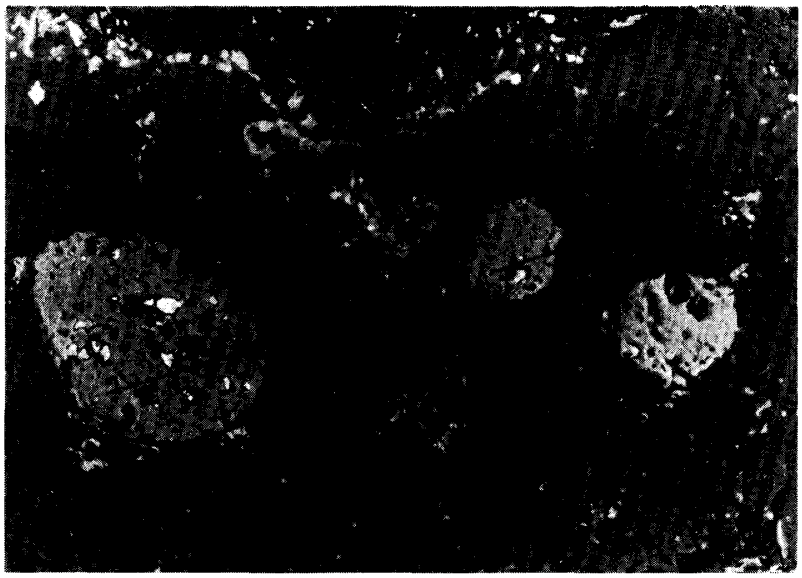

Fig. 41. Opaque spherules mainly magnetite (gray), associated with patches of pentlandite and troilite (white). Yamato (c). Reflected light. ×350.

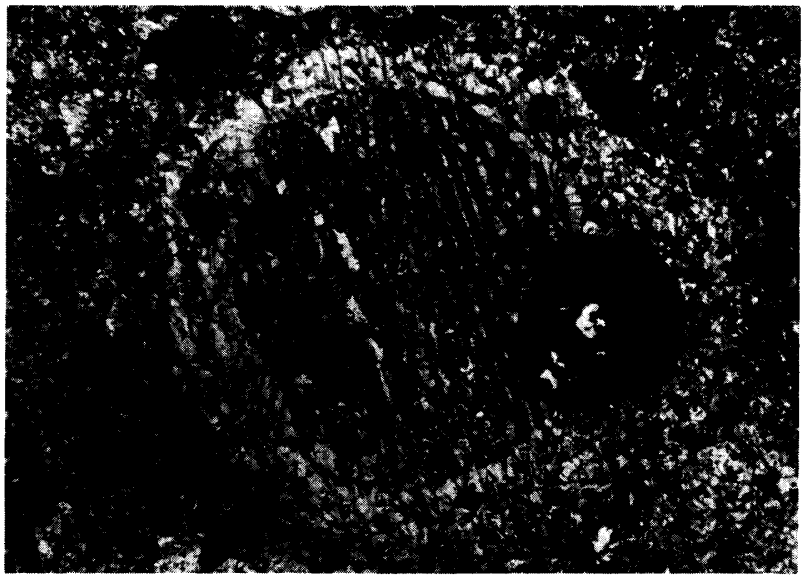

Fig. 42. An olivine chondrule joined with a rounded grain of magnetite in the margin. Yamato(c). Transmitted light. ×51.

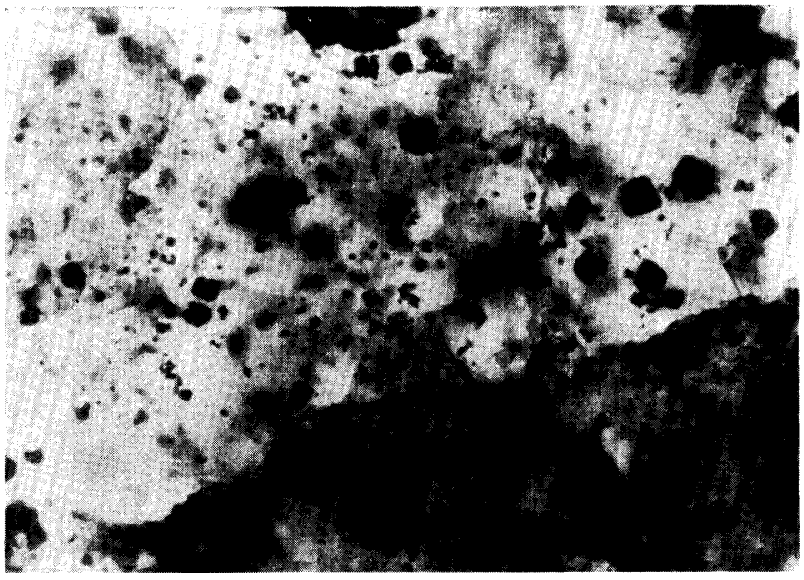

Fig. 43. Minute idiomorphic grains of magnetite and spinel-like crystals included in plagioclase. Cubic form of grains is common. Yamato (c). Transmitted light. ×570.

Fig. 44. Thin needle-like crystals of clinopyroxene occurring in plagioclase. Yamato (c). Transmitted light. ×460.

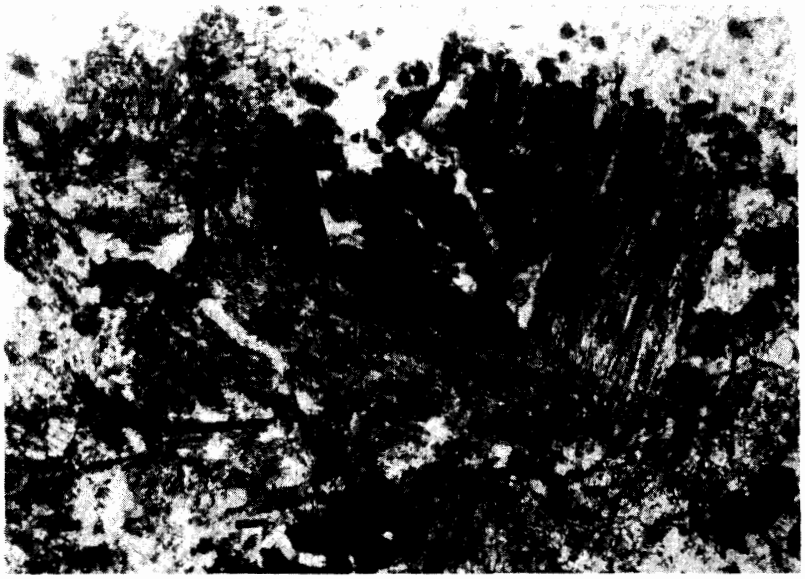

Fig. 45. An extremely sheared orthopyroxene grain in the matrix. Yamato (c). Transmitted light. ×63.

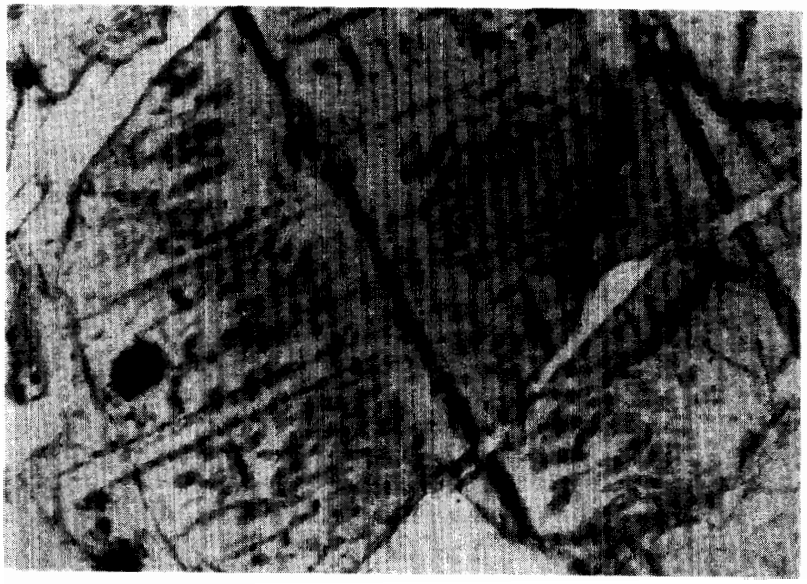

Fig. 46. Minute greenish brown inclusions in olivine. They occur nearly in parallel to the crystal axes of olivine. Yamato (c). Transmitted light. ×350.

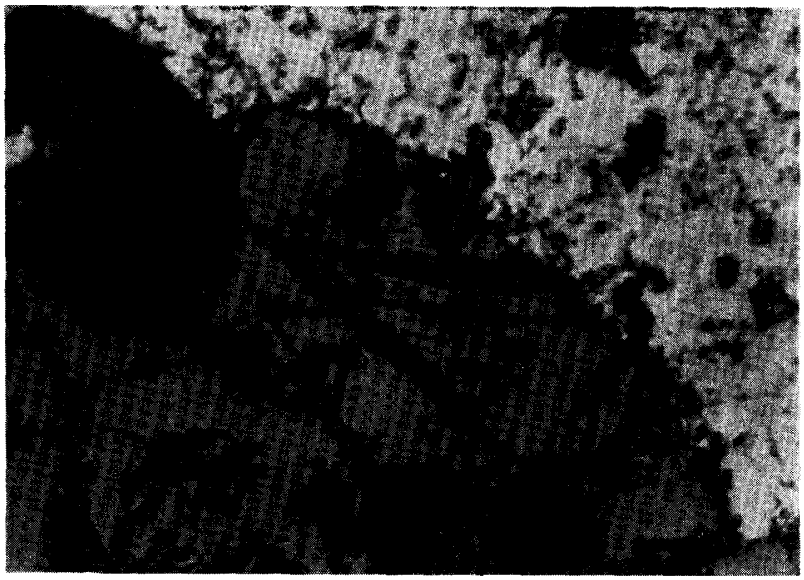

Fig. 47. Exsolution lamellae of ilmenite (dark gray) in host magnetite (gray). Yamato (c). Reflected light. ×570.

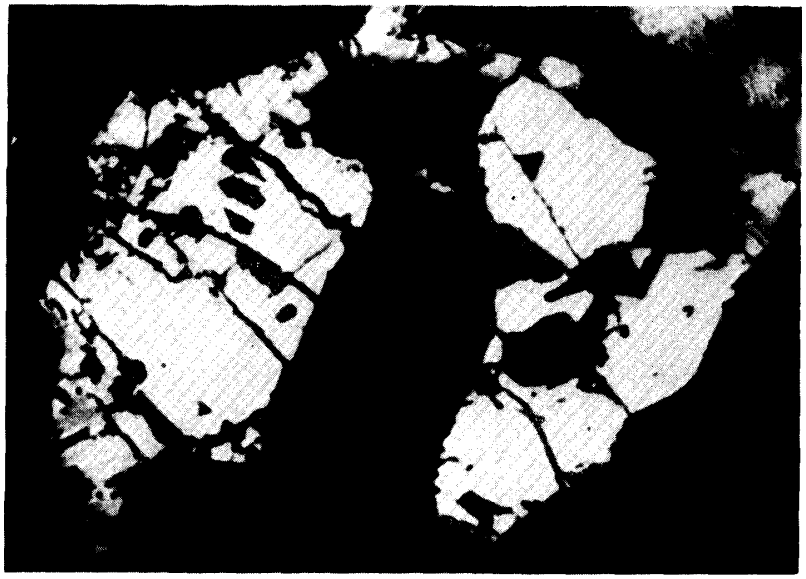

Fig. 48. Idiomorphic pentlandite crystals exhibiting distinct cleavages. Yamato (c). Reflected light. ×800.

Fig. 49. Intergrowth of pentlandite (light gray) and troilite (gray). This grain includes fine, irregular patches of nickel-iron (white). Yamato(c). Reflected light. ×1600.

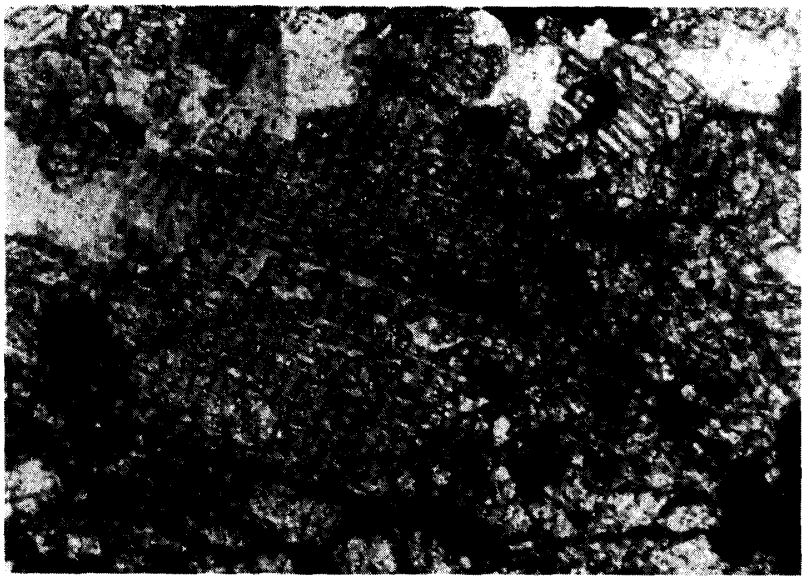

Fig. 50. A thin section of the Yamato (d) meteorite. This meteorite is chondritic. Chondrules are small in number, and the boundary between chondrule and matrix is less distinct. Transmitted light. ×110.

Fig. 51. Minute troilite droplets associated with partially fused silicate vein. Yamato (d). Reflected light. ×630.

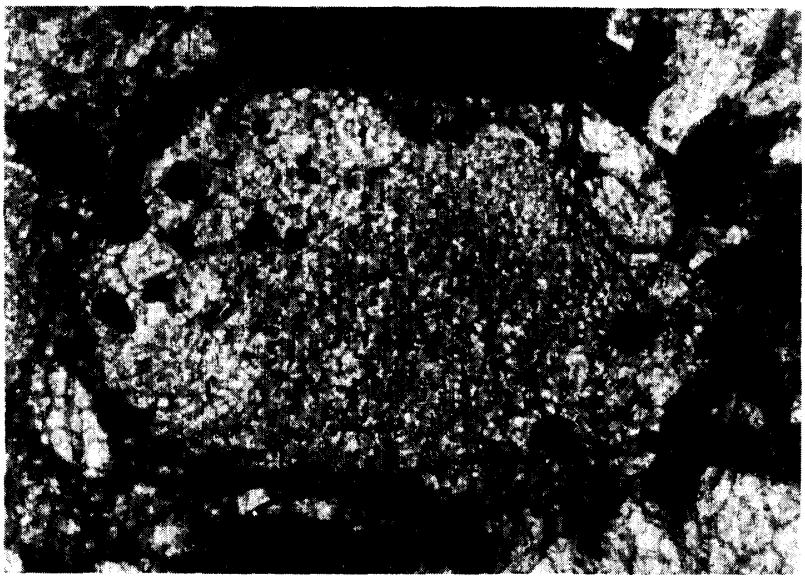

Fig. 52. An olivine crystal grading into fine grains, retaining the original euhedral form. Yamato (d). Transmitted light. ×120.

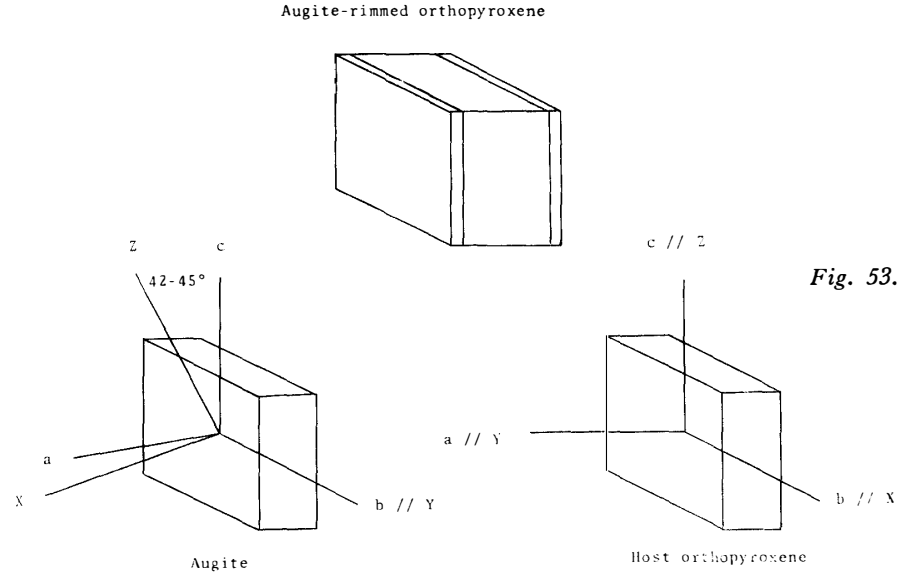

Fig. 53. The arrangement of optical and crystallographic axes of host orthopyroxene and surrounding augite.

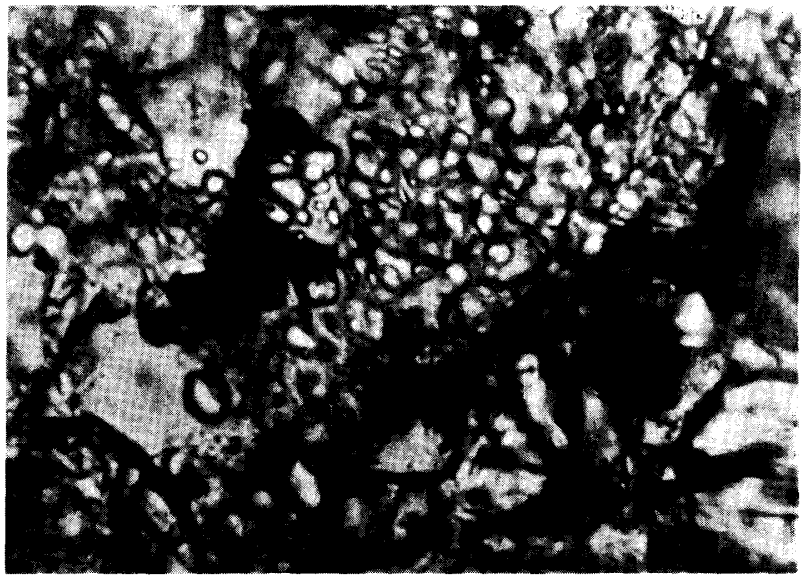

Fig. 54. Silicate droplets (probably pyroxene) in plagioclase in contact with orthopyroxene. Yamato (d). Transmitted light. ×690.

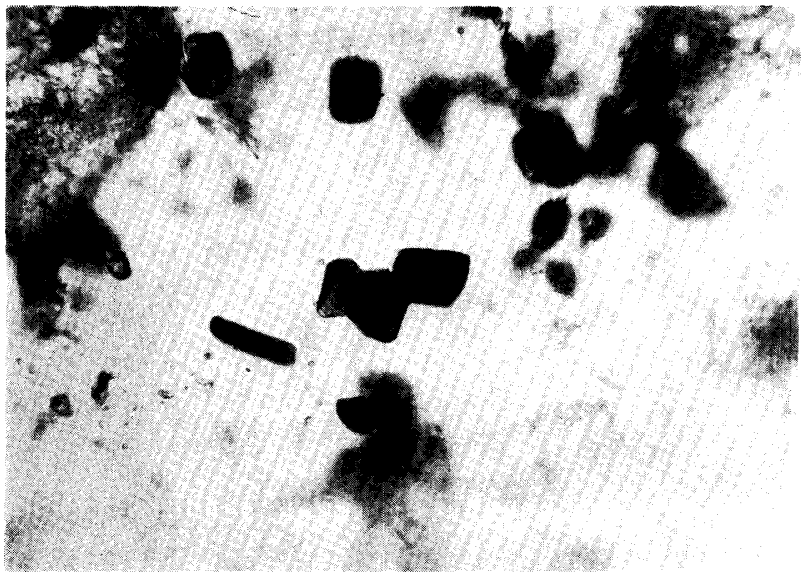

Fig. 55. Idiomorphic, spinel-like grains in plagioclase. Yamato (d). Transmitted light. ×800.

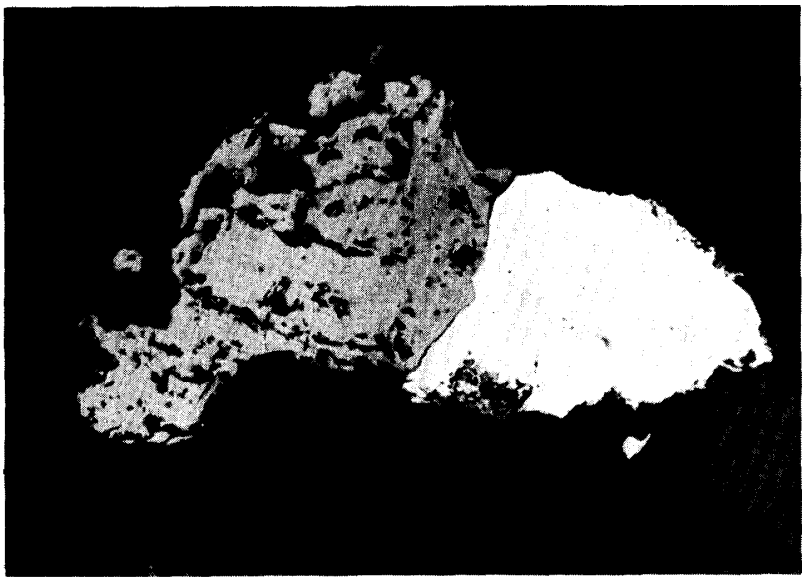

Fig. 56. Intergrowth of nickel-iron (white) and troilite (light gray). Yamato (d). Reflected light. ×270.

Fig. 57. Intergrowth of kamacite (light gray) and taenite (white). Yamato (d). Reflected light. ×970.

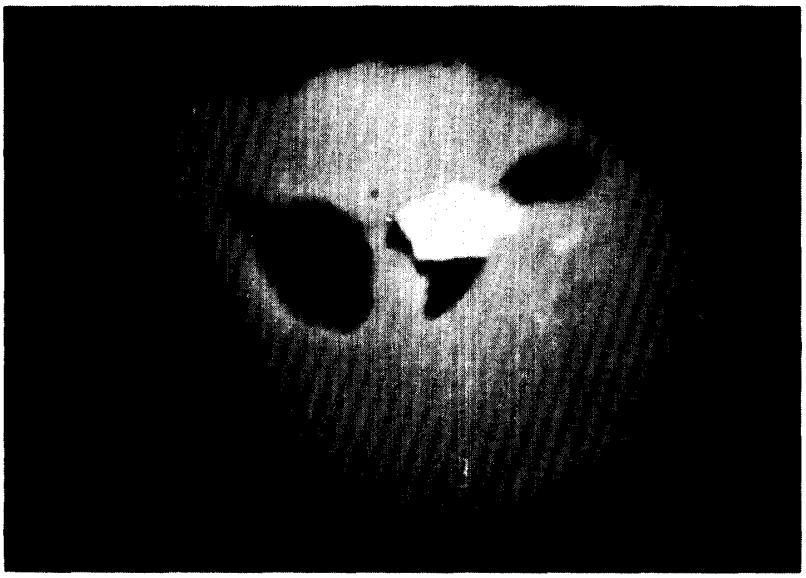

Fig. 58. Native copper (white) associated with troilite (black grains in this photograph) in kamacite (dark gray). This photograph was taken using a strong red filter. Yamato(d). Reflected light. ×1700.

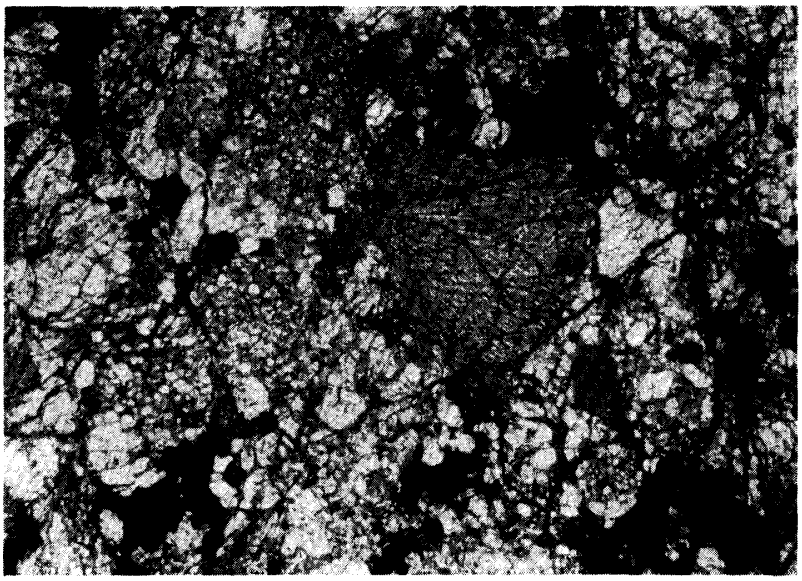

Fig. 59. A thin section of the Yamato (g) meteorite. Chondritic structure is notable in this meteorite, but chondrules are generally deformed from the spheroidal and ellipsoidal forms. Yamato (g). Transmitted light. ×34.

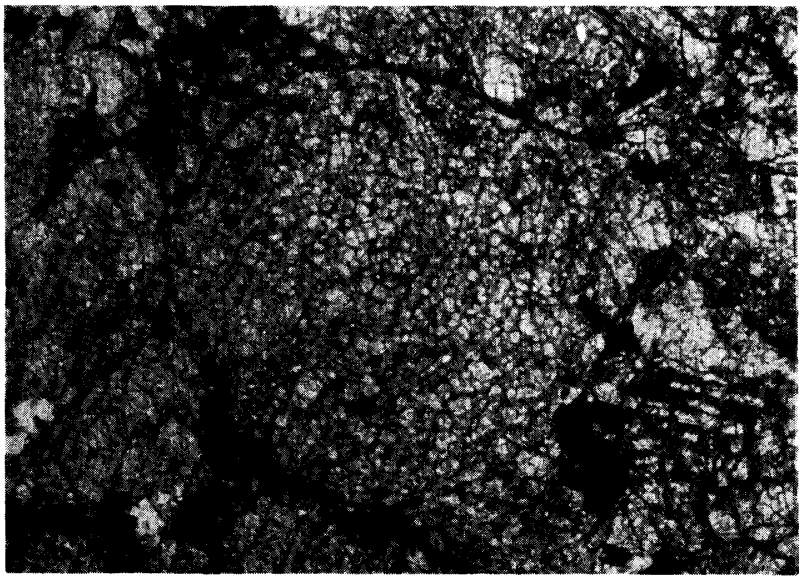

Fig. 60. A granular chondrule composed entirely of minute olivine grains. Yamato (g). Transmitted light. ×40.

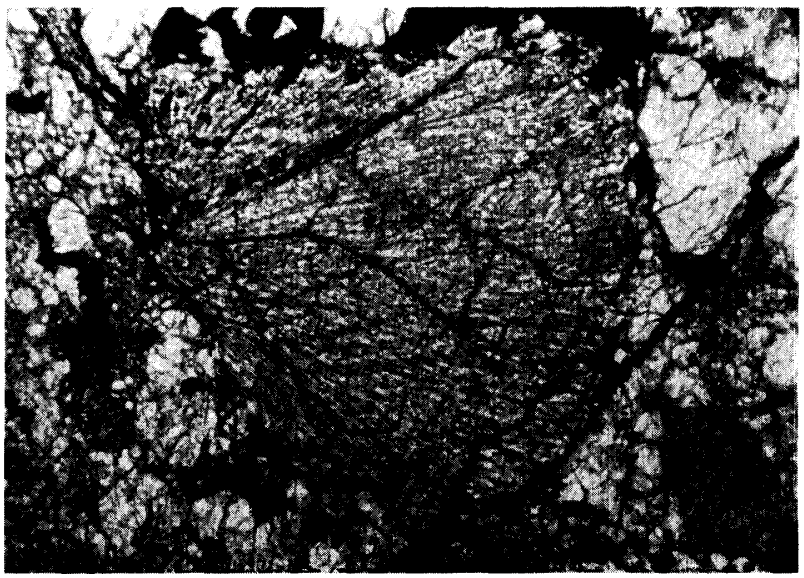

Fig. 61. A radiating orthopyroxene chondrule. Yamato (g). Transmitted light. ×74.

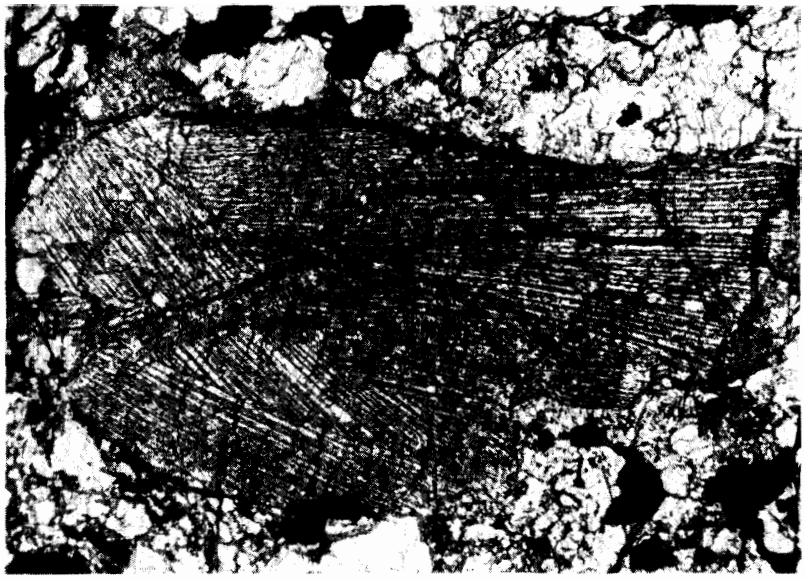

Fig. 62. A radiating chondrule consisting mainly of fibrous olivine crystals interstitially filled with clinopyroxene. This chondrule has remarkably deformed appearance. Yamato (g). Transmitted light. ×57.

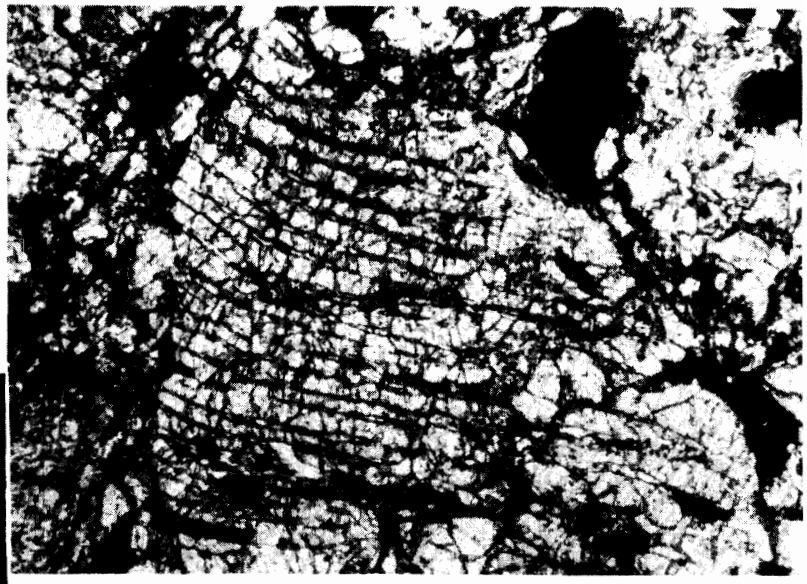

Fig. 63. A barred chondrule consisting of rod-like olivine. Yamato (g). Transmitted light. ×19.

Fig. 64. Exsolution lamellae of clinopyroxene in augite which is a reaction rim of orthopyroxene. Yamato (g). Transmitted light. Nicol crossed. ×690.

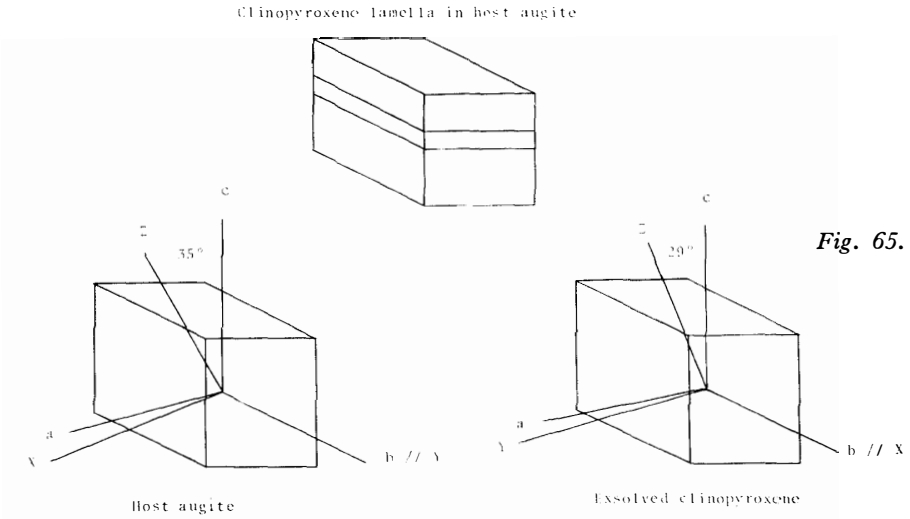

Fig. 65. The arrangement of optical and crystallographic axes of host augite and lamellar clinopyroxene.

Fig. 66. Orthopyroxene with a kink band associated with exsolution lamellae of clinopyroxene. The kink band is distinguishable by the slightly inclined extinction in the orthopyroxene grain. Yamato (g). Transmitted light. Nicol crossed. ×860.

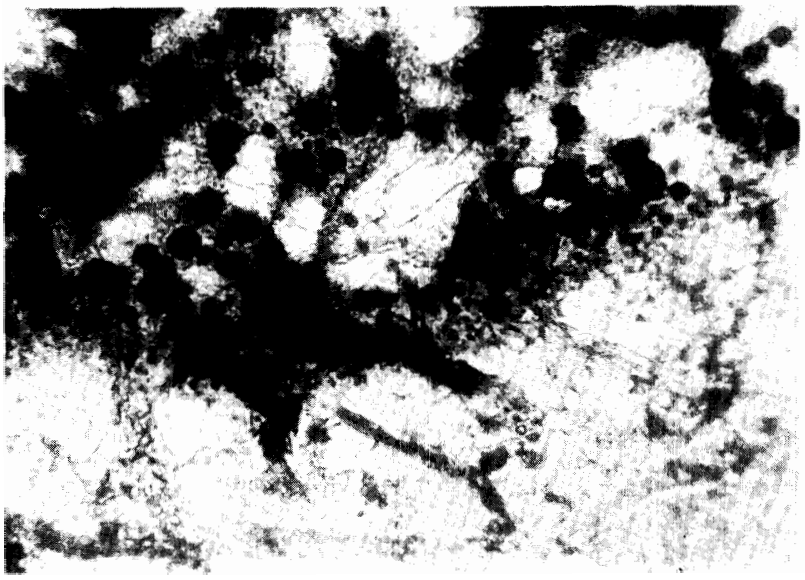

Fig. 67. Opaque fused droplets distributed along the dark-colored, fused silicate vein. Yamato (g). Transmitted light. ×290.